https://dx.doi.org/10.1016/j.tre.2022.102999

Stochastic ridesharing equilibrium problem with compensation optimization

Tongfei Li [a], Min Xu [b], Huijun Sun [c], Jie Xiong [a], Xueping Dou [a]

[a] Beijing Key Laboratory of Traffic Engineering, Beijing University of Technology, Beijing 100124, China

[b] Department of Industrial and Systems Engineering, The Hong Kong Polytechnic University, Hung Hom, Hong Kong, China

[c] Key Laboratory of Transport Industry of Big Data Application Technologies for Comprehensive Transport, Ministry of Transport, Beijing Jiaotong University, Beijing 100044, China

Abstract

In the urban traffic system with the introduction of ridesharing programs, we develop a path-based generalized stochastic user equilibrium model to formulate travelers' mode and route choice behavior. To suit more general scenarios, the proposed model takes into consideration of travelers' heterogeneity in terms of car ownership and value of time, and travelers' limited perceived ability based on the stochastic user equilibrium principle instead of Wardrop's user equilibrium principle. Moreover, it can overcome inherent shortcomings of link-based formulation, i.e., path information of travelers cannot be tracked, travelers are allowed to change mode choices for a single trip, etc. The proposed model is formulated as variational inequalities and an equivalent mixed complementarity problem due to the inseparable and asymmetric travel cost functions. Furthermore, we address a decision-making problem of ridesharing compensation from the perspective of traffic managers and policy-makers who want to achieve total travel cost minimization and vehicular air pollution emissions minimization simultaneously. A bi-objective bi-level optimization model is proposed to formulate this leader-follower hierarchical decision-making problem, in which travelers' mode and route choice behavior has been respected. It is further reformulated as a mathematical problem with complementarity constraints and solved by an improved Non-Dominated Sorting Genetic Algorithm II to generate a set of Pareto-optimal solutions for policy-makers and allow them to choose desired solutions. Finally, several numerical experiments based on two different-scale networks are conducted to demonstrate the properties of the problem, the performance of our established model and the proposed algorithm. The results show that rational pricing of ridesharing compensation can indeed improve urban traffic congestions and pollution emissions simultaneously. Moreover, by integrating travelers' choice behavior based on the SUE principle instead of the UE principle in the ridesharing compensation optimization model, this study derives a series of more effective decision-making strategies of ridesharing compensation.

Keywords: Ridesharing; emerging travel mode; stochastic user equilibrium; ridesharing compensation; traffic policy

1 Introduction

With the development of sharing economy, ridesharing, as an emerging travel mode, becomes more and more popular all over the world. A number of transportation network companies (e.g., Uber, Lyft, Grab, and Didi) have emerged to provide on-demand dynamic ridesharing services for users. Comparing with other sharing mobility services (e.g., car-sharing, bike-sharing), ridesharing is a "real" sharing mobility service based on social vehicle resources without increasing the number of car ownership. Specifically, on the supply side, they allow drivers to share vacant seats with others who have similar itineraries so as to sharing car-related expenses. On the demand side, each ridesharing rider should pay a certain sum of compensation to the driver for providing ridesharing services according to a pre-specified pricing scheme. Comparing with driving alone, ridesharing riders can enjoy a similar door-to-door travel experience with much lower travel expenses, while they do not have to bear the high cost of owning a private vehicle and worry about parking issues. Note that both ride-hailing and ridesharing can provide efficient on-demand services for riders by the smartphone-based rider service application, however, they are two different emerging transportation services. Ride-hailing services (also called ride-sourcing) are provided by dedicated drivers who behave like taxi drivers for pursuing profit, while ridesharing is a non-profit travel service provided by non-dedicated drivers who want to share car-related expenses during commuting time based on their private vehicles, such as UberPool, Lyft Line, and DiDi Hitch. Ridesharing can realize the optimal combination of social vehicle resources, make full use of vehicle idle capacity (i.e., raise vehicle occupancy), and finally reduce overall car use (Furuhata et al., 2013; Wang et al., 2018; Long et al., 2018; Coulombel et al., 2019). Previous studies illustrated that for one additional passenger per 100 vehicles, annual CO2 emissions in the U.S. would be reduced by almost 7.2 million tons (Concas and Winters, 2007; Jacobson and King, 2009; Caulfield, 2009). Accordingly, comparing with the incentive transportation infrastructure investment, ridesharing programs are widely recognized as a novel efficient method to relieve traffic congestions and reduce vehicular air pollution emissions caused by the high private car ownership rate and the high percentage of people driving alone in big cities (Concas and Winters, 2007; Jacobson and King, 2009; Caulfield, 2009; Coulombel et al., 2019).

As an emerging travel mode enhancing urban mobility, the introduction of ridesharing programs in the existing transportation network significantly reshapes travelers' mode and route choice behavior at the individual level, the spatiotemporal distribution of traffic congestion, and vehicular air pollution emissions at the aggregate level. Meanwhile, the aggregated impacts of ridesharing programs on the urban traffic system are the primary concern of traffic managers and policy-makers in the presence of ridesharing, because exploring their interrelationship can be used to appraise the performance of ridesharing programs and further help assist traffic managers in making policy and regulation decisions regarding ridesharing services (Li et al., 2020).

To explore the aggregated impacts of ridesharing programs on urban traffic congestions, the related literature can be classified into two different categories according to the research methodology: theoretical research (Xu, Ordóñez and Dessouky, 2015; Xu, Pang, Ordónez and Dessouky, 2015; Liu and Li, 2017; Di et al., 2018; Wang et al., 2018; Wang, Ban and Huang, 2019; Li et al., 2020; Ma et al., 2020) and empirical research (Nielsen et al., 2015; Chen, 2018; Wang, Chen and Chen, 2019). From the perspective of theoretical research, researchers pursue establishing a

rigorous mathematical modeling framework to formulate the new traffic distribution based on the analysis of travelers' choice behavior (i.e., travel mode choice, route choice, commuting time choice) in the presence of ridesharing. Moreover, the formulation of travelers' choice behavior in all literature is based on Wardrop's user equilibrium (UE) principle (Wardrop, 1952). Under the premise of taking ridesharing as a new travel mode, Xu et al. (2015) extends the classic traffic assignment model with elastic demand to formulate the interrelationship between ridesharing programs and traffic congestions. For simplify, they adopt an aggregate model to analyze the number of travelers chosen different modes for each origin-destination (OD) pair and do not treat each traveler as an individual agent. Specifically, the individual choice behavior among different travel modes is not considered. In contrast, the number of ridesharing drivers and ridesharing riders is exogenously given. All of them only make a decision on whether to travel or not. Later, Xu et al. (2015) further relaxes the previous assumption that drivers and riders sharing the same vehicle must share the same OD in Xu et al. (2015) and formulates the travelers' choice behavior at the individual level as a mixed complementarity problem. The number of ridesharing drivers and ridesharing riders is endogenous according to the principle of self-utility maximization rather than exogenously given in Xu et al. (2015). To reduce the problem size and facilitate computation, Di et al. (2018) reformulates Xu et al. (2015)'s model to a link-node based ridesharing user equilibrium formulation which avoids path enumeration and thus is more suit for large-scale transportation networks. However, due to the inherent shortcoming of the link-based ridesharing user equilibrium model in the aforementioned studies (Xu, Pang, Ordónez and Dessouky, 2015; Di et al., 2018), one ridesharing rider needs to take several ridesharing vehicles (i.e., several transfers) for a single trip and the routing information of the matched ridesharing riders and ridesharing drivers cannot be tracked. To overcome this problem, based on the assumption that a single ridesharing driver can only pick up one rider (i.e., single driver single rider), Li Yuanyuan et al. (2020) further proposes a path-based equilibrium model to formulate the decision-making problem of travelers in the presence of ridesharing programs, which can track the matching and routing decisions of the matched drivers and riders. In addition, there are some studies focus on the morning commute problem in the presence of ridesharing programs which can be used to explore the temporal distribution of traffic congestions, the commuters' choices of departure time and travel mode (among solo drivers, ridesharing drivers, and ridesharing riders) are explained as dynamic UE with the setting of fixed-ration charging-compensation scheme (Liu and Li, 2017) or the variable-ratio charging-compensation scheme (Wang, Ban and Huang, 2019). However, all the above studies (Xu, Ordóñez and Dessouky, 2015; Xu, Pang, Ordónez and Dessouky, 2015; Di et al., 2018; Ma et al., 2020) assume each traveler owns a private vehicle and he/she can freely switch the role among different traffic modes. Moreover, public transit which is the main travel mode of non-car owners in reality does not take into account. Based on the assumption that one ridesharing driver can only pick up one rider (i.e., single driver single rider), Wang xiaolei et al. (2018) firstly divides all travelers into two different categories in terms of their car ownership (i.e., car owners and non-car owners). Then, a variational inequality model is established to explore the mode choice of heterogeneous travelers at UE. However, the assumption of single driver single rider significantly limited its practical utility. From the perspective of empirical research, there are few literatures dedicated to using various data resources (e.g., questionnaire survey data, self-collected operation data, etc.) to analyze the impact of ridesharing programs

on peoples' travel mode choices (Nielsen et al., 2015; Chen, 2018; Wang, Chen and Chen, 2019). Nielsen et al. (2015) explores Danish perceptions about organization-based ridesharing based on original research collected through semi-structured research interviews and five focus groups throughout Denmark. Based on the self-collected census-tract data, Chen Yefu (2018) analyzed the effect of ridesharing on the travel mode choice in Seattle through the difference-in-differences analysis and the K-mean Cluster analysis. Wang Ze et al. (2019) collects a total of 607 survey data via the DiDi platform and analyzes the young people's ridesharing behavior characteristics and behavioral impacts in Hangzhou, China.

The extent to which ridesharing reduces vehicular emissions has been analyzed theoretically and empirically by few studies at a different level of spatial aggregation (i.e., city, state, and country). Jacobson and King (2009) propose a mathematical model to estimate the emissions reduction due to the introduction of ridesharing programs in the U.S. They find that if one additional passenger is added in per 100 vehicles or per 10 vehicles, annual CO2 emissions will be reduced by almost 7.2 and 68.0 million tons, respectively. Focusing on an individual town, Caulfield (2009) finds that ridesharing can save 12,500 tons of CO2 annually in Dublin, Ireland. Javid et al. (2017) firstly develops a multiple regression model to analyze ridesharing propensity in all 50 U.S. states and the District of Columbia. Then, they quantify the extent to which increasing HOV lane-kilometers would lead to reductions in vehicular air pollution emissions across the U.S., by state. However, all the literature is the statistics and analysis of the impact of ridesharing services on vehicular emissions based on the currently collected data rather than the optimization of vehicular emissions in the urban traffic system with ridesharing services.

As mentioned above, the introduction of ridesharing programs provides an emerging travel mode for all travelers, which can significantly affect urban traffic congestions and vehicular air pollution emissions by changing travelers' mode and route choice behavior. Despite the importance of ridesharing compensation to travelers' mode choice in the urban system with ridesharing, the pricing problem of ridesharing compensation has not been explicitly studied yet. Based on the established variational inequality model, the nonlinear complementarity model, or the fixed point model that is used to formulated travelers' mode choice at UE in the presence of ridesharing programs, all the limited studies adopt the method of sensitivity analysis to analyze the impacts of ridesharing compensation on travelers' mode choice at the individual level and traffic congestions at the aggregate level (Wang et al., 2018; Xu, Pang, Ordónez and Dessouky, 2015; Yan et al., 2019). Another stream of related literature focuses on how to employ surge/dynamic pricing techniques to increase the matching rate of ridesharing services in the daily operation and mitigate the impact of temporal/spatial demand fluctuations on service (Liu and Li, 2017; Wang, Ban and Huang, 2019; Bimpikis et al., 2019).

The pricing of ridesharing compensation directly affects the decision-making of peoples' travel mode and route choices at the individual level, and further affects urban traffic congestions and vehicular air pollution emissions at the aggregate level. Meanwhile, different from ride-hailing services, ridesharing services are a not-for-profit industry. Naturally, for traffic managers and policy-makers, the pricing of ridesharing compensation can be an effective way and management strategy to relieve traffic congestions and reduce vehicular air pollution emissions. This paper aims to provide a general model to formulate travelers' mode and route choice behav-

ior in the presence of ridesharing programs. Then, based on the analysis on the interrelationship between the ridesharing compensation and the travelers' mode and route choice behavior, we further focuses on the decision-making problem of ridesharing compensation from the perspective of traffic managers and policy-makers. This study contributes to the state-of-the-art transportation management and policy-making in the presence of ridesharing programs as follows:

First, we develop a path-based generalized stochastic user equilibrium model to formulate travelers' mode and route choice behavior. Different from the existing ridesharing studies based on Wardrop's user equilibrium (UE) principle (Xu, Ordóñez and Dessouky, 2015; Xu, Pang, Ordónez and Dessouky, 2015; Liu and Li, 2017; Di et al., 2018; Wang et al., 2018), our model explicitly considers the stochastic factors caused by the limited perceived ability of travelers and formulates their choice behavior based on the stochastic user equilibrium (SUE) principle. That makes our formulation is more consistent with reality and suitable for more general scenarios because UE is just a special case of SUE. Moreover, the path-based modeling method makes it possible to overcome inherent shortcomings of link-based formulation, i.e., path information of travelers cannot be tracked, one ridesharing rider can take several ridesharing vehicles in turns for a single trip., etc. Besides, due to the inseparable and asymmetric travel cost functions, the proposed model is formulated as variational inequalities and an equivalent mixed complementarity problem that enables us to efficiently calculate its solutions.

Second, there is a lack of an explicit mathematical optimization model for the decision-making problem of ridesharing compensation in the urban traffic system with the introduction of ridesharing programs. A limited number of previous studies (Wang et al., 2018; Xu, Pang, Ordónez and Dessouky, 2015; Yan et al., 2019) adopt the method of sensitivity analysis to analyze the impact of ridesharing compensation on urban traffic conditions. To fill the research gap, we develop a rigorous mathematical model (i.e., a bi-objective bi-level programming model) with the integration of travelers' mode and route choice behavior to optimize the ridesharing compensation. Namely, the demand of travelers choosing each travel mode (i.e., solo drivers, ridesharing drivers, ridesharing riders, and public transit riders) and each path in the optimization model is endogenously determined which depends on the travelers' mode and route choices. It provides a more general and efficient methodology for the decision-making problem of ridesharing compensation. Moreover, because total travel cost minimization and vehicular air pollution emissions minimization are differently measured and scaled objectives that policy-makers want to achieve, an improved Non-Dominated Sorting Genetic Algorithm II is proposed to generate a set of Pareto-optimal solutions instead of one single solution. Besides, we also analyze the impact of subsidy policy on urban traffic conditions and pollution emissions in the early days of ridesharing.

Third, compared with previous related studies (Xu, Ordóñez and Dessouky, 2015; Xu, Pang, Ordónez and Dessouky, 2015; Liu and Li, 2017; Di et al., 2018; Ma et al., 2020), the proposed model takes into consideration of travelers' heterogeneity. Specifically, we relax the assumption that each traveler owns a private vehicle to the more realistic scenario where travelers are heterogeneous in terms of car ownership and value of time (VOT). All travelers can be classified into two categories: car owners with higher VOT and non-car owners with lower VOT. They choose travel modes available in their own category. Furthermore, as one of the main travel modes of non-car owners, public transit is considered in the formulation which has always been neglected

by previous studies except for Wang's work (Wang et al., 2018). However, we extend Wang's study to a more general form by considering the single driver multi-riders scenario and endogenous traffic congestions rather than the constant travel cost. As for the calculation of travelers' travel costs, occupancy rates of the ridesharing vehicle are variable depends on the travel flow of ridesharing drivers and riders rather than a constant (Xu, Pang, Ordónez and Dessouky, 2015; Li and Liu, 2020). Namely, the generalized travel cost of each ridesharing driver is related to the average number of ridesharing riders it carries in reality.

This paper is structured as follows. In Section 2, we give a detailed description of the urban traffic system in the presence of ridesharing programs, and the considered optimization problem. Then, the technology of problem reformulation with the assistance of an extended network is used to the modeling of the original optimization problem. In Section 3, a bi-objective bi-level programming model is established and reformulated to solve the compensation optimization problem. In Section 4, an improved Non-Dominated Sorting Genetic Algorithm II with the combination of CONOPT solver of GAMS is proposed to generate Pareto optimal alternatives. In Section 5, a set of numerical experiments is conducted to demonstrate the properties of the problem. Section 6 provides concluding remarks.

2 Notations, modeling setting, problem statement and reformulation

2.1 Description of urban traffic systems with the introduction of ridesharing services

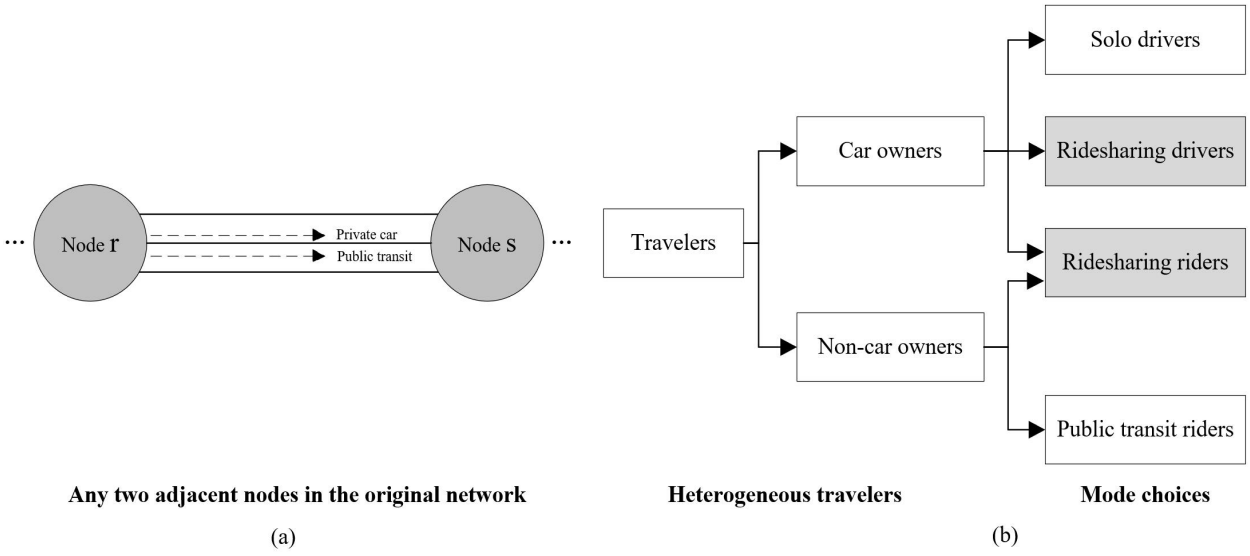

Figure 1: Urban traffic system with ridesharing services and heterogeneous travelers

In this study, we consider an urban traffic system in the presence of ridesharing programs. Through the emerging ridesharing platform (e.g., UberPool, Lyft Line, DiDi Hitch), private vehicles can participate in the ridesharing system to supply ridesharing services by sharing vacant seats with others who have similar itineraries. A private vehicle with a single driver can pick up multiple riders within the vehicle's capacity. In the process of actual operation, each rideshar-

ing rider should pay a certain sum of money to the ridesharing driver who shares a ride with him/her according to a pre-specified pricing scheme. For ridesharing drivers, the payment paid by each rider is compensation to them for supplying ridesharing services that will cover part of their travel expenses. Moreover, both drivers and riders in the ridesharing system will tolerate the additional inconvenience cost caused by sharing a vehicle with other travelers. The cost of picking up, dropping off, waiting time, and the uncomfortable cost of sharing the interior space of a vehicle with strangers are included in the inconvenience cost. Accordingly, the inconvenience cost is positively correlated with the occupancy rate of ridesharing vehicles. Besides, compared with ride-hailing, ridesharing systems have no dedicated drivers, therefore, all travelers have the freedom to join or leave the ridesharing market based on their individual preferences.

For the purpose of illustration, a general traffic network is considered in this study. In the traffic network, each origin node can be regarded as a residential area, and each destination node can be regarded as a workplace. There are a road a and a public transit line b that runs in parallel between any two adjacent nodes as shown in Figure 1(a). Due to the limited road capacity, travelers on road a will suffer traffic congestions caused by the increase of vehicle flows. The public transit vehicle operates on the public transit line b according to the pre-scheduled timetable with fixed headway (e.g., bus rapid transit line, urban rail transit line). Moreover, its running time between residential area and workplace is a constant, which is not affected by the increase of public transit riders and traffic congestions on road a. As for travelers who choose public transit, they arrive at the public transit station evenly and board the public transit vehicle on a first-come-first-serve basis. Because each public transit vehicle has a limited capacity, travelers have to wait at the public transit station for the next public transit vehicle if the current vehicle is fully loaded with riders. Here, we assume the basic attribute of roads and public transit lines in the traffic network is known.

Meanwhile, there are many travelers who commute from residential locations to workplaces through different routes every day. Due to the difference in affordability and individual preferences, not all travelers own a private vehicle. Travelers are heterogeneous in terms of their car ownership. Assuming the car ownership is known and travelers do not change their car ownership in the short-run (Wang et al., 2018), all travelers can be classified into two categories: car owners and non-car owners. Compared with non-car owners, car owners generally have higher affordability and more care about the consumed time during commuting, therefore, car owners have a higher VOT. As described above, in the urban traffic system with the introduction of ridesharing programs, there are four travel modes as follows: solo driving, participating in the ridesharing system as drivers, participating in the ridesharing system as riders, taking the public transit. Every day, all travelers choose among travel modes available in their own category as shown in Figure 1(b) and do not change their mode choices during traveling. Here, it is assumed that car-use habits make car owners always choose to use the car instead of the public transit during commuting trips (Gärling and Steg, 2007). Specifically, for the daily commute, car owners can choose to drive alone, travel as ridesharing drivers, or travel as ridesharing riders, while non-car owners can choose to travel as ridesharing riders or ride public transit.

2.2 Problem statement

There are two decision-makers whose strategies are highly correlated with each other in the urban traffic system. The first one is heterogenous travelers who make mode and route choice decisions according to their perception of the external traffic condition every day. The other one is traffic managers and policy-makers who make the decisions of ridesharing compensation to achieve total travel cost minimization and vehicular air pollution emissions minimization. Because the change of ridesharing compensation directly determines the cost that travelers participate in ridesharing programs, it will significantly change travelers' mode and route choice behavior at the individual level, and in return travelers' mode and route choice further affect the total travel cost and vehicular air pollution emissions at the aggregate level. The complex interrelationship among urban traffic conditions, vehicular air pollution emissions, heterogenous travelers' mode and route choice behavior, and ridesharing compensation makes it difficult to determine the optimal ridesharing compensation with respect to the whole urban traffic system. In this study, we focus on the decision-making problem of the ridesharing compensation to appraise the performance of ridesharing programs and further help assist traffic managers in making policy and regulation decisions regarding ridesharing services, in which the travelers' mode choice behavior and route choice behavior must be respected.

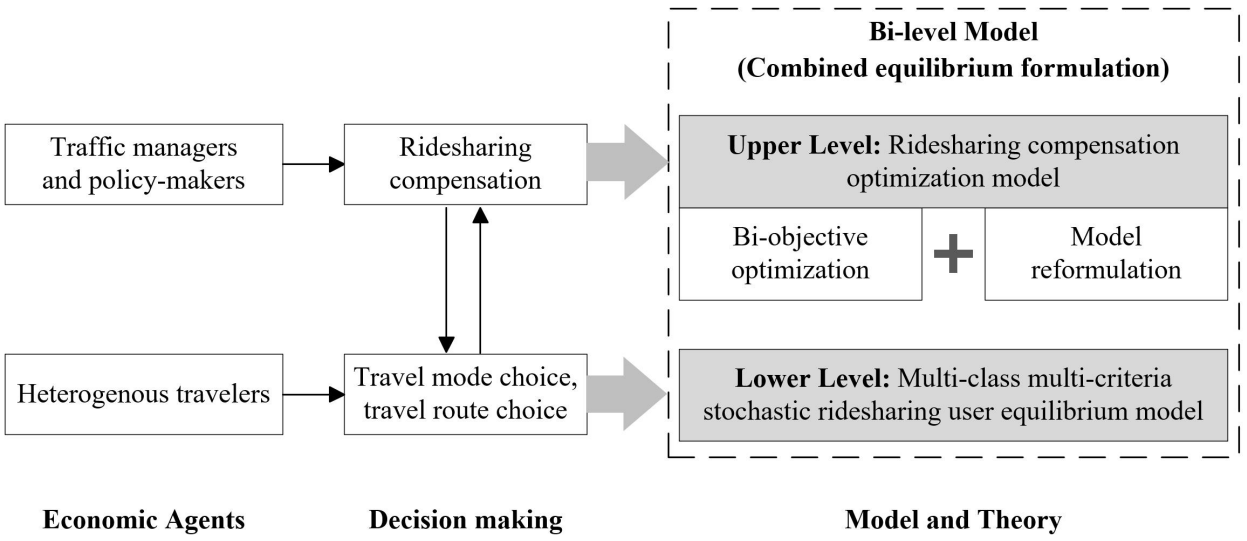

Figure 2: Framework of this study

According to the analysis of the interrelationship between travelers and traffic managers, we can know they are two decision-makers at two different levels, and the proposed problem is a leader-follower hierarchical decision-making problem that can be formulated as a bi-level programming model. As shown in Figure 2, the upper-level decision-makers are traffic managers and policy-makers, and the lower-level decision-makers are heterogeneous travelers. As for the upper-level, traffic managers and policy-makers want to achieve two different goals at the same time by making the decision of ridesharing compensation.

As for the lower-level, heterogeneous travelers make the travel mode and route choice decisions in the presence of ridesharing programs. As rational travelers, they will have a comprehen-

sive consideration on the travel time cost, the monetary cost, and other costs of each travel mode and each route when they make mode and route choice decisions. However, due to the limited perceived ability, travelers can not perceive the actual travel cost of each mode choice and each route choice exactly. Therefore, each rational traveler chooses a travel mode and a route to minimize his/her own expected value of the perceived generalized travel cost due to the existence of perceptual errors. The choosing process of each traveler can be regarded as an independent decision-making action, and thus the collective mode and route choice behavior in the presence of ridesharing programs can be viewed as a non-corporative game. However, due to the cross-group externalities among solo drivers, ridesharing drivers, ridesharing riders, and public transit riders, travelers who choose different travel modes and routes have a mutual influence on each other and the impact is reflected by the change of the individual generalized travel cost. The number of travelers who choose each travel mode and each route, and the generalized travel cost of each travel mode and each route are endogenous during this interactive process. Eventually, all travelers who belong to different categories can find the best mode and route choices to minimize their individual expected value of the perceived generalized travel costs (include travel time cost, monetary cost, etc). Therefore, we should address the combined travel mode and route choice problem with multi-user classes in the presence of ridesharing programs.

2.3 Problem reformulation and model setting

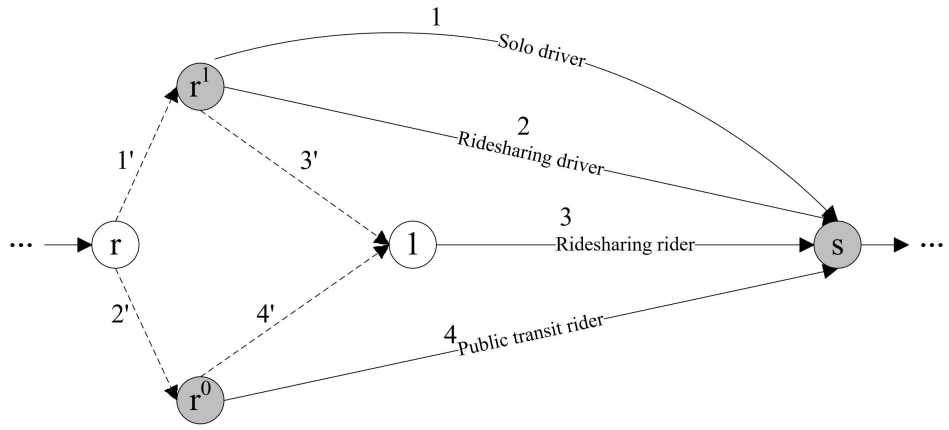

Figure 3: Construction of the extended network

Before modeling the decision-making problem of ridesharing compensation which is bi-level programming, the lower-level model should be established firstly. The technology of problem reformulation with the assistance of an extended network is used to model the combined travel mode and route choice problem with multi-user classes for the original network in Figure 1(a). Thus, as solutions of the combined travel mode and route choice problem, mode-specific flows and path flows for car owners and non-car owners (i.e., the number of heterogeneous travelers choose each mode and each path) at SUE in the original network can be visually displayed in an extended network by manipulating a graphical representation method.

(1) Construction of the extended network

As shown in Figure 3, node r, s denote any two adjacent nodes in the original network. Node r is the original node, while node s is the destination node. Because all travelers can be classified into two categories and travelers belong to different categories have different options available on travel mode choices, we separate the original node r into two nodes r^1, r^0 and add them between adjacent nodes r, s. Then, connect nodes r^1, r^0 with the original node r by two dummy links $a_{1'}, a_{2'}$ with zero travel cost respectively. Meanwhile, keep the destination node s unchanged. To visualize different mode choices of heterogeneous travelers, we construct three paths between nodes r^1, s and two paths between nodes r^0, s. Specifically, since both car-owners and non-car owners can choose travel as ridesharing riders, one node (node 1) is added between nodes $r^1 s$, nodes $r^0 s$. Both node r^1 and node r^0 are connected with node 1 by the dummy link (i.e., link $a_{3'}$ and link $a_{4'}$) with zero travel cost. Node 1 is further connected with the destination node s by a solid link a_3. Thus, node r^1 are connected with the destination node s by two solid links a_1, a_2 directly and one path passes through dummy link $a_{3'}$, node 1, and solid link a_3 successively, while node r^0 are connected with the destination node s by one solid links a_3 directly and one path passes through dummy link $a_{4'}$, node 1, and solid link a_3 successively. For all adjacent nodes in the original network, implement the same process as illustrated in Figure 3. Finally, we can construct an extended network for the original network.

From the perspective of topology, in the extended network, the original node r is connected with node r^1 and node r^0 which illustrates all travelers pass through the adjacent nodes r, s in the original network can be classified into car owners and non-car owners. Thus, r^1, r^0 represent car owners' origin node and non-car owners' origin node respectively. Specifically, the travel demand between any OD pair can be classified into the travel demand of car owners and the travel demand of non-car owners. For the travel demand of car owners from origin r to any destination in the original network, its original node is node r^1, and its destination is unchanged in the extended network. Similarly, for the travel demand of non-car owners from origin r to any destination in the original network, its original node is node r^0, and its destination is unchanged in the extended network. Note that the travel demand distribution of car owners and non-car owners in the original network is exogenously given and known. Besides, paths between node r^1 and node s are the visualization of different mode choices for car owners (i.e., solo drivers, ridesharing drivers, and ridesharing riders), while paths between node r^0 and node s are the visualization of different mode choices for non-car owners (i.e., ridesharing rider and public transit rider). Thus, the path flow represents the number of car owners or non-car owners who choose a certain travel mode and a certain path pass through the adjacent nodes r, s in the original network. Furthermore, there are four travel modes in the urban system with the introduction of ridesharing programs as described in Section 2.1. All of them are illustrated by solid links between each OD pair in the extended network of Figure 3. Thus, traffic flow on each solid link represents the number of travelers who choose a certain travel mode.

(2) Model setting

In the extended network of Figure 3, let R^1 denote the set of car owners' origin nodes, $r^1 \in R^1$. R^0 denotes the set of non-car owners' origin nodes, $r^0 \in R^1$. S is the set of destination nodes, $s \in S$. a represents a link in the original network, while b is a public transit line that runs in parallel with link a between the same OD pair. $K = \{1, 2, 3, 4\}$ represent different travel modes

which are visualized by solid links, $k \in K$. Let A_k denote the set of solid links indicate travel model k, $a_k \in A_k$. Each solid link indicates one travel mode in turns: solo divers (i.e., link a_1), ridesharing drivers (i.e., link a_2), ridesharing riders (i.e., link a_3), and public transit riders (i.e., link a_4). x_{a_k} represents the travel flow on link a_k, which means the number of travelers who choose travel mode k, $k \in K$ passes through link a in the original network.

Meanwhile, P^{rs} is the set of paths between OD pair rs in the original network, $p^{rs} \in P^{rs}$. Note that rs represents an arbitrary OD pair in the original network rather than being limited to adjacent nodes as described in the above subsection. $K^1 = \{1, 2, 3\}$ and $K^0 = \{3, 4\}$ represent a set of travel modes that can be chosen by car owners or non-car owners respectively. Let $P_k^{r^1s}$ denote the set of paths between OD pair r^1s for car owners who choose travel mode k. $p_k^{r^1s}$ is a path in set $P_k^{r^1s}$, it has $p_k^{r^1s} \in P_k^{r^1s}$. Similarly, $P_k^{r^0s}$ denotes the set of paths between OD pair r^0s for non-car owners choose travel mode k^0, $p_{k^0}^{r^0s} \in P_k^{r^0s}$. r^1s, r^0s denote two OD pairs in the extended network corresponding to OD pair rs in the original network. Let $f_{p_k^{r^1s}}$ denote the travel flow on path $p_k^{r^1s}$, which means the number of car owners choose travel mode k on path p^{rs} in the original network. $C_{p_k^{r^1s}}$ denotes the travel cost of path $p_k^{r^1s}$, which means the travel cost of travel mode k^1 on path p^{rs} for car owners. Similarly, from the perspective of non-car owners, let $f_{p_k^{r^0s}}$ and $C_{p_k^{r^0s}}$ denote the travel flow on path $p_k^{r^0s}$ and the travel cost of path $p_k^{r^0s}$ respectively.

In order to show the mutual corresponding relations intuitively, the relationship and meaning of OD pairs, travelers, and paths in the original and extended network are listed in Table 1.

Table 1: Travelers, OD pairs, and set of paths in the original and extended network

Original network				Extended network	
OD pair	Set of paths	Travelers	Travel modes	OD pairs	Set of paths
rs	P^{rs}	Car owners	Solo driver	r^1s	$P_1^{r^1s}$
			Ridesharing driver		$P_2^{r^1s}$
			Ridesharing rider		$P_3^{r^1s}$
		Non-car owners	Ridesharing driver	r^0s	$P_3^{r^0s}$
			Public transit rider		$P_4^{r^0s}$

Note. r^1 and r^0 are two nodes in the extended network, which corresponding to the same origin node r in the original network.

In the extended network, the relationship between link flow x_{a_k} and path plow $f_{p_{k1}^{r^1s}}, f_{p_{k^0}^{r^0s}}$ is listed as follows:

$$x_{a_k} = \begin{cases} \sum_{r^1 \in R^1} \sum_{s \in S} \sum_{p_k^{r^1s} \in P_k^{r^1s}} f_{p_k^{r^1s}} \delta_{a_k p_k^{r^1s}} & \text{if } k \in K^1,\ k \neq 3 \\ \sum_{r^1 \in R^1} \sum_{s \in S} \sum_{p_k^{r^1s} \in P_k^{r^1s}} f_{p_k^{r^1s}} \delta_{a_k p_k^{r^1s}} + \sum_{r^0 \in R^0} \sum_{s \in S} \sum_{p_k^{r^0s} \in P_k^{r^0s}} f_{p_k^{r^0s}} \delta_{a_k p_{k^0}^{r^0s}} & \text{if } k = 3 \\ \sum_{r^0 \in R^0} \sum_{s \in S} \sum_{p_k^{r^0s} \in P_k^{r^0s}} f_{p_k^{r^0s}} \delta_{a_k p_k^{r^0s}} & \text{if } k \in K^0,\ k \neq 3 \end{cases} \tag{1}$$

where $\delta_{a_k p_{k1}^{r^1 s}}$ and $\delta_{a_k p_k^{r^0 s}}$ are binary variables. $\delta_{a_k p_k^{r^1 s}} = 1$ $\left(\delta_{a_k p_k^{r^0 s}} = 1\right)$ when link a_k is on the path $p_{k1}^{r^1 s}$ $\left(p_k^{r^0 s}\right)$ between OD pair $r^1 s$ $\left(r^0 s\right)$. Otherwise, $\delta_{a_k p_k^{r^1 s}} = 0$ $\left(\delta_{a_k p_k^{r^0 s}} = 0\right)$. The amount of link flow x_{a_k} is equal to the sum of the flows of all paths passing through link a_k. Note that the second equality in the above equation indicates that because both car owners and non-car owners can travel as ridesharing riders, the number of ridesharing riders pass through link a equals to the sum of the number of car owners who travel as ridesharing riders pass through link a and the number of non-car owners who travel as ridesharing riders pass through link a.

In the original network as shown in Figure 1(a), there are two classes of traffic flow: the vehicle flow and the travel flow. Both of them will be taken into consideration when calculating the travel cost on the congested road. Let x_a denote the vehicle flow on road a, and x_b denote the travel flow on public transit line b. Since $b \in B$ is a public transit line that runs in parallel with road a between the same OD pair. x_a and x_b have the following relationship with link flows x_{a_k} in the extended network:

$$\begin{cases} x_a = x_{a_1} + x_{a_2} & \text{Vehicle flow on road } a \\ x_b = x_{a_4} & \text{Travel flow on public transit line } b \end{cases} \tag{2}$$

The first equality indicates that vehicle flow on road a (i.e., x_a) equals to the sum of the number of solo drivers x_{a_1} and ridesharing drivers x_{a_2} on road a. In the second equality, both x_b and x_{a_4} represent the number of public transit riders on public transit line b.

Besides, the free-flow travel time and capacity of link a_k in the extended network equal to the free-flow travel time and capacity of link a in the original network except link a_4 which represents the public transit line. Let t_a^0, c_a denote the free-flow travel time and capacity of road a. t_b^0, c_b denote the fixed running time and capacity of public transit vehicles on line b. Thus, after defining $t_{a_k}^0, c_{a_k}$ represent the free-flow travel time and capacity of link a_k in the extended network, it has:

$$\begin{cases} t_{a_k}^0 = t_a^0,\ c_{a_k} = c_a, & \forall k \in K^1 \\ t_{a_4}^0 = t_b^0,\ c_{a_4} = c_b \end{cases} \tag{3}$$

Finally, mode-specific flows and path flows for car owners and non-car owners at SUE which are solutions of the combined travel mode and route choice problem for the original network in the presence of ridesharing services are visually represented by the path flow between each OD pair $\left\{f_{p_k^{r^1 s}}, f_{p_k^{r^0 s}},\ \forall r^1 \in R^1, r^0 \in R^0, s \in S, k \in K\right\}$ in the extended network as shown in Figure 3.

By constructing an extended network as shown in Figure 3, we transform the combined travel mode and route choice problem (i.e., the lower-level programming problem of bi-level model as illustrated in Figure 2) in the presence of ridesharing programs for the original network in Figure 1(a) into an equivalent route choice problem for the extended network in Figure 3. Accordingly, the equivalent route choice problem for the extended network in Figure 3 can be further formulated and solved as a stochastic traffic assignment problem in the following section. To formulate the model mathematically, the notations used in this study are listed in Table 2.

Table 2: List of Parameters and Decision Variables

Parameters and General Variables

A:	Set of roads in the original network, $a \in A$;
B:	Set of public transit lines in the original network, $b \in B$ is a public transit line that run in parallel with road a between the same OD pair;
R:	Set of original nodes in the original network;
t_a^0, t_b^0:	Free-flow travel time of road a, fixed running time of the public transit vehicle on line b;
c_a, c_b:	Capacity of road a, capacity of public transit vehicles on line b;
H_b:	Departure headway of public transit line b;
τ^{PT}:	Fare cost for riders on public transit line;
x_a, x_b:	Vehicle flow on road a, travel flow on public transit line b;
P^{rs}:	Set of paths between OD pair rs in the original network;
R^1, R^0:	Set of car owners' or non-car owners' origin nodes in the extended network, $r^1 \in R^1, r^0 \in R^1$;
S:	Set of destination nodes in the original and extended network, $s \in S$;
K^1, K^0:	Set of travel modes can be choose by car owners or non-car owners, $K^1 = \{1,2,3\}, K^0 = \{3,4\}$;
A_k:	Set of solid links that indicate travel model k in the extended network, $a_k \in A_k$;
$t_{a_k}^0$:	Free-flow travel time of link a_k in the extended network;
c_{a_k}:	Capacity of link a_k in the extended network;
$P_k^{r^1 s}, P_k^{r^0 s}$:	Set of paths between OD pair $r^1 s$ or $r^0 s$ for travelers choose mode k in the extended network, $p_k^{r^1 s} \in P_k^{r^1 s}$, $p^{r^0 s} \in P_k^{r^0 s}$;
x_{a_k}:	Travel flow on link a_k in the extended network;
$\delta_{a_k p_k^{r^1 s}}, \delta_{a_k p_k^{r^0 s}}$:	Binary variables. They equal to 1 when link a_k is on the path $p_k^{r^1 s}$ or $p_k^{r^0 s}$. Otherwise, $\delta_{a_k p_k^{r^1 s}} = 0, \delta_{a_k p_k^{r^0 s}} = 0$;
$C_{p_k^{rs}}, \tilde{C}_{p_k^{rs}}$:	Travel cost of path p_k^{rs}, generalized travel cost of path p_k^{rs};
$q^{r^1 s}, q^{r^0 s}$:	Travel demand of car owners between OD pair $r^1 s$, travel demand of non-car owners between OD pair $r^0 s$;
α, β:	Parameters of the BPR function;
η_1, η_0:	Value of time (VOT) of car owners and non-car owners;
h:	Vehicle fuel cost per hour;
Δ:	Inconvenience cost caused by sharing a vehicle with others;
$v_{p^{rs}}$:	Average occupancy rate of each ridesharing vehicle between OD pair rs in the original network;
Cap:	Capacity of each ridesharing vehicle;
θ:	Parameter of the perceptual error in the logit-based stochastic route choice model;
$\varepsilon_1, \varepsilon_2$:	Parameters in the vehicular emission function.

Decision variables

τ^{rs}:	Ridesharing compensation/payment between OD pair rs in the original network;
$\boldsymbol{\tau}$:	Vector of ridesharing compensations/payments, $\boldsymbol{\tau} = \{\tau^{rs}, \ \forall r \in R, s \in S\}$;
$f_{p_{k^1}^{r^1 s}}, f_{p_{k^0}^{r^0 s}}$:	Travel flow on path $p_{k^1}^{r^1 s}$ or $p_{k^0}^{r^0 s}$ in the extended network;
$\mathbf{f}$:	Vector of path flow, $\mathbf{f} = \left\{ f_{p_k^{r^1 s}}, f_{p_k^{r^0 s}}, \ \forall r^1 \in R^1, r^0 \in R^0, s \in S, k \in K \right\}$;
$\lambda_+^{p^{rs}}, \lambda_-^{p^{rs}}$:	Lagrangian multipliers for the lower bound constraint and the upper bound constraint on path p^{rs} between OD pair rs respectively;
$\boldsymbol{\lambda}$:	Vector of Lagrangian multipliers, $\boldsymbol{\lambda} = \{\lambda_+^{rs}, \lambda_-^{rs}, \ \forall r \in R, s \in S\}$.

3 Optimization model

In this section, a bi-objective bi-level optimization model is proposed to formulate and solve the decision-making problem of ridesharing compensation. First, an asymmetric stochastic traffic assignment model with side constraints and multi-user classes is established to formulate the route choice problem in the extended network based on the nonlinear complementarity approach. Then, a bi-objective function combined with two different objectives is proposed. Finally, after presenting the complete ridesharing compensation optimization model where the established stochastic traffic assignment model is the lower-level model, we convert the bi-objective bi-level optimization model into a bi-objective single-level nonlinear programming problem.

3.1 Travel cost function

As described in Section 2.1, there are four travel modes in the urban system with the introduction of ridesharing programs: solo drivers, ridesharing drivers, ridesharing riders, and public transit riders. However, heterogeneous travelers can only choose among travel modes available in their own category. The composition of travel cost for each travel mode and constraints for path flow will be introduced in the following subsection.

3.1.1 Travel cost consideration in the original network

Specifically, the composition of the travel cost on road a for different mode choices and public transit line b in the original network is defined and calculated as follows:

Travel time on road a: All travelers on road a (i.e., solo drivers, ridesharing drivers, ridesharing riders) suffer travel time cost. Due to the limited road capacity, traffic congestions caused by the raise of vehicle flows should be taken into consideration. Here, the BPR (Bureau of Public Roads) function is used to calculate the travel time on the congestion rod a as follows:

$$t_a = t_a^0 \left[1 + \alpha \left(\frac{x_a}{c_a} \right)^{\beta} \right], \quad \forall a \in A \tag{4}$$

where t_a is the travel time on road a. t_a^0 is the free-flow travel time on road a, and c_a is the capacity of road a. x_a, the vehicle flow on road a, equals to the sum of the number of solo drivers and the number of ridesharing drivers on road a as shown in Eq.(2). α and β are two parameters.

Fuel cost for solo drivers and ridesharing drivers on road a: As owners of private vehicles, both solo drivers and ridesharing drivers should bear the fuel cost of daily commuting. h is the fuel cost per hour of private vehicles which is measured in monetary units. Therefore, the fuel cost for solo drivers and ridesharing drivers travel through road a equals to $t_a h$.

Ridesharing payment for ridesharing riders on road a: Besides the travel time cost, as described in Section 2.1, each ridesharing rider should pay a certain sum of money τ^{rs} to the ridesharing driver who shares a ride with him/her from origin r to destination s according to a pre-specified pricing scheme. Thus, τ^{rs} is the ridesharing payment for each ridesharing rider between OD pair rs. Generally, it is determined according to a pre-specified pricing scheme.

Ridesharing compensation for ridesharing drivers on road a: Because a ridesharing driver can pick up multiple riders and each rider should pay a certain sum of money to the driver, the total

payment paid by all riders on the same ridesharing vehicle can be regarded as the total compensation for the ridesharing driver and cover part of the driver's car-related expenses. Naturally, the ridesharing compensation is in direct proportion to the number of riders on the ridesharing vehicle (i.e., the number of riders that the ridesharing driver picks up). Let $v_{p^{rs}}$ denote the average occupancy rate of each ridesharing vehicle on path p^{rs} between OD pair rs (i.e., the average number of riders that each ridesharing driver picks up on path p^{rs} from origin r to destination s). Note that we assume all travelers do not change their travel modes, and ridesharing riders do not change ridesharing vehicles during the one-time commuting (Li et al., 2020), therefore, average occupancy rate $v_{p^{rs}}$ is a path-based measure rather than a link-based measure. τ^{rs} denotes the ridesharing payment paid by each ridesharing rider between OD pair rs which is also the compensation that a ridesharing driver received for picking up one rider. Thus, the ridesharing compensation for a ridesharing driver on path p^{rs} between OD pair rs is $v_{p^{rs}}\tau^{rs}$.

Inconvenience cost for ridesharing drivers and ridesharing riders on road a: Besides travel time costs, both ridesharing drivers and ridesharing riders will tolerate the additional inconvenience cost caused by sharing a ride with others. The time cost of picking up and dropping off, waiting time cost, and the uncomfortable cost of sharing the interior space of a vehicle with strangers are measured in monetary units and included in the inconvenience cost. Naturally, the inconvenience cost is in direct proportion to the average occupancy rate of each ridesharing vehicle. Δ is the inconvenience cost caused by sharing a ride with one additional traveler. Therefore, the inconvenience cost for each ridesharing driver and each ridesharing rider on path p^{rs} between OD pair rs is $v_{p^{rs}}\Delta$.

Travel time on public transit line b: Because the running time of the public transit vehicle between each OD pair is constant, public transit riders spend fixed travel time after boarding the public transit vehicle. Let t_b^0 denote the fixed running time of public transit vehicle on line b.

Waiting time on public transit line b: Besides the fixed running time, public transit riders will experience an extra waiting time at their originating station before boarding caused by excessive passengers and the limited capacity of public transit vehicles. The public transit vehicle operates on line b according to the pre-scheduled timetable with fixed headway H_b. If riders' originating station is the origin node of line b, based on the assumption travelers arrive at the station evenly and board the public transit vehicle on a FCFS basis, the average waiting time can be calculated as follows:

$$w_b = \frac{1}{2} H_b \frac{x_b}{c_b}, \quad \forall b \in B \tag{5}$$

where w_b is the average waiting time of public transit riders on public transit line b. H_b denotes the departure headway of the public transit line b. c_b denotes the capacity of public transit vehicles. x_b is the travel flow on public transit line b.

Fare cost on the public transit line: Besides the waiting time cost and running time cost on the public transit line, each public transit rider should pay for the fare. τ^{PT} denotes the fare cost on public transit line in monetary units.

3.1.2 Travel cost consideration in the extended network

In Section 3.1.1, the composition of travel cost for each mode choice in the original network is listed in detail. According to the physical meaning of the path travel cost in Section 2.3, travel

cost functions of each path between OD pair r^1s and r^0s in the extended network of Figure 3 can be calculated one by one. Furthermore, each path travel cost function can be further expressed as a function of the path flow according to the relationship between the path flow and the link flow in Eq.(1). Namely, the path-based formulation of travel cost is used in this study.

(1) Path travel cost in the extended network

Specifically, the path travel cost of each path between OD pair r^1s and r^0s in the extended network is defined and calculated as follows:

Travel cost of path $p_1^{r^1s}$ (Solo drivers): Let $C_{p_1^{r^1s}}$ denote the travel cost of path $p_1^{r^1s}$ in the extended network, which represents the travel cost of solo drivers on path p^{rs} in the original network. As described in Section 3.1.1, solo drivers have to bear the travel time cost and the fuel cost during daily commuting. Therefore, the travel cost of path $p_1^{r^1s}$ is equal to the sum of travel time cost and fuel cost on links of path $p_1^{r^1s}$ as follows:

$$C_{p_1^{r^1s}} = \sum_{a_1 \in A_1} t_{a_1}^0 \left[1 + \alpha \left(\frac{x_{a_1} + x_{a_2}}{c_{a_1}}\right)^{\beta}\right] (\eta_1 + h)\, \delta_{a_1 p_1^{r^1s}}, \quad \forall p_1^{r^1s} \in P_1^{r^1s}, r^1 \in R^1, s \in S \tag{6}$$

where η_1 is the VOT of car owners. It converts the travel time into monetary units. According to Eqs.(1-2), we can know that $x_{a_1} + x_{a_2} = x_a$ represents the vehicle flow on link a. a_2 is a solid link which represents ridesharing drivers during the same OD pair with link a_1 in the extended network of Figure 3.

Travel cost of path $p_2^{r^1s}$ (Ridesharing drivers): Besides the travel time cost and the fuel cost, ridesharing drivers also tolerate the additional inconvenience cost. Meanwhile, the ridesharing compensation paid by riders can cover part of their car-related expenses. Thus, the travel cost of path $p_2^{r^1s}$ can be calculated as follows:

$$C_{p_2^{r^1s}} = \sum_{a_2 \in A_2} t_{a_2}^0 \left[1 + \alpha \left(\frac{x_{a_1} + x_{a_2}}{c_{a_2}}\right)^{\beta}\right] (\eta_1 + h)\, \delta_{a_2 p_2^{r^1s}} + v_{p^{rs}} (\Delta - \tau^{rs}), \quad \forall p_2^{r^1s} \in P_2^{r^1s}, r \in R, s \in S \tag{7}$$

where $v_{p^{rs}}$ is the average occupancy rate of each ridesharing vehicle on path p^{rs} between OD pair rs. According to the physical meaning of path flow, it can be calculated as follows:

$$v_{p^{rs}} = \frac{f_{p_3^{r^1s}} + f_{p_3^{r^0s}}}{f_{p_2^{r^1s}}}, \quad \forall p^{rs} \in P^{rs}, r \in R, s \in S \tag{8}$$

where the numerator $f_{p_3^{r^1s}} + f_{p_3^{r^0s}}$ is the number of ridesharing riders on path p^{rs} between OD pair rs, and the denominator $f_{p_2^{r^1s}}$ is the number of ridesharing vehicles (i.e., the number of ridesharing drivers) on path p^{rs} between OD pair rs.

Travel cost of path $p_3^{r^1s}$ (Ridesharing riders for car owners): Let $C_{p_3^{r^1s}}$ denote the travel cost of path $p_3^{r^1s}$ in the extended network, which represents the travel cost of car owners who travel as ridesharing riders on path p^{rs} in the original network. Car owners who participate in the ridesharing system as ridesharing riders will suffer the travel time cost, the inconvenience cost, and the monetary cost caused by the ridesharing payment paid to the ridesharing driver. There-

fore, the travel cost of path $p_3^{r^1 s}$ can be calculated as follows:

$$C_{p_3^{r^1 s}} = \sum_{a_3 \in A_3} t_{a_3}^0 \left[1 + \alpha \left(\frac{x_{a_1} + x_{a_2}}{c_{a_3}} \right)^{\beta} \right] \eta_1 \delta_{a_3 p_3^{r^1 s}} + v_{p^{rs}} \Delta + \tau^{rs}, \quad \forall p_3^{r^1 s} \in P_3^{r^1 s}, r \in R, s \in S \tag{9}$$

Travel cost of path $p_3^{r^0 s}$ (Ridesharing riders for non-car owners): Similarly, $C_{p_3^{r^0 s}}$ denotes the travel cost of path $p_3^{r^0 s}$ in the extended network, which represents the travel cost of non-car owners who travel as ridesharing riders on path p^{rs} in the original network. As ridesharing riders, non-car owners have the same components of travel cost as car owners. η_0 denotes the VOT of non-car owners. As described in Section 2.1, the VOT of car owners is higher than VOT of non-car owners, i.e., $\eta_1 > \eta_0$. Therefore, the travel cost of path $p_3^{r^0 s}$ can be calculated as follows:

$$C_{p_3^{r^0 s}} = \sum_{a_3 \in A_3} t_{a_3}^0 \left[1 + \alpha \left(\frac{x_{a_1} + x_{a_2}}{c_{a_3}} \right)^{\beta} \right] \eta_0 \delta_{a_3 p_3^{r^0 s}} + v_{p^{rs}} \Delta + \tau^{rs}, \quad \forall p_3^{r^0 s} \in P_3^{r^0 s}, r \in R, s \in S \tag{10}$$

Travel cost of path $p_4^{r^0 s}$ (Public transit riders): Let $C_{p_4^{r^0 s}}$ denote the travel cost of path $p_4^{r^0 s}$ in the extended network, which represents the travel cost of non-car owners who travel as public transit riders. When travelers choose public transit to travel, they will suffer the waiting time cost, the fixed running time cost, and the fare cost. Therefore, the travel cost of path $p_4^{r^0 s}$ can be calculated as follows:

$$C_{p_4^{r^0 s}} = \sum_{a_4 \in A_4} \left(\frac{1}{2} H_{a_4} \frac{x_{a_4}}{c_{a_4}} \delta_{r^0 a_4} + t_{a_4}^0 \right) \eta_0 \delta_{a_4 p_4^{r^0 s}} + \tau^{PT}, \quad \forall p_4^{r^0 s} \in P_4^{r^0 s}, r^0 \in R^0, s \in S \tag{11}$$

where $\delta_{r^0 a_4}$ is a binary variable. $\delta_{r^0 a_4} = 1$ when public transit riders' originating station is the origin node of link a_4, and $\delta_{r^0 a_4} = 0$ otherwise. Because $b \in B$ is the public transit line that run in parallel with road a between the same OD pair in the original network, we have $H_{a_4} = H_b$ and $c_{a_4} = c_b$.

(2) Path constraints

As the solution of stochastic traffic assignment problem in the extended network of Figure 3, path flow $\left\{ f_{p_k^{r^1 s}}, f_{p_k^{r^0 s}}, \ \forall r^1 \in R^1, r^0 \in R^0, s \in S, k \in K \right\}$ should satisfy the following constraints.

Demand constraints: In the extended network, the sum of path flows between OD pair $r^1 s$, $r^0 s$ should be equal to the travel demand of OD pair $r^1 s$ and $r^0 s$ respectively. It indicates the sum of the number of car owners (non-car owners) who choose each travel mode is equal to the number (i.e., travel demand) of car owners (non-car owners) in the original network.

$$\sum_{k \in K^1} \sum_{p_k^{r^1 s} \in P_k^{r^1 s}} f_{p_k^{r^1 s}} = q^{r^1 s}, \quad \forall r^1 \in R^1, s \in S \tag{12}$$

$$\sum_{k \in K^0} \sum_{p_k^{r^0 s} \in P_k^{r^0 s}} f_{p_k^{r^0 s}} = q^{r^0 s}, \quad \forall r^0 \in R^0, s \in S \tag{13}$$

where $q^{r^1 s}$ and $q^{r^1 s}$ are the travel demand of car owners and non-car owners between OD pare rs in the original network. They are exogenously given and known.

Non-negative constraints: As the path flow or the number of travelers choose a certain travel mode, $f_{p_k^{rs}}$ should be non-negative.

$$f_{p_k^{r^1s}} \geq 0, \quad \forall p_k^{r^1s} \in P_k^{r^1s}, r^1 \in R^1, s \in S, k \in K^1 \tag{14}$$

$$f_{p_k^{r^0s}} \geq 0, \quad \forall p_k^{r^0s} \in P_k^{r^0s}, r^0 \in R^0, s \in S, k \in K^0 \tag{15}$$

Except for the above constraints, according to the physical meaning of path flows (i.e., the number of travelers who choose certain travel modes) as described in Section 2.3, two additional constraints on path flow $f_{p_k^{rs}}$ which can represent the distinct features of ridesharing programs should also be satisfied.

Lower bound constraint: Each ridesharing driver should pick up at least one ridesharing rider, otherwise, he/she can only travel as solo drivers rather than ridesharing drivers. Thus, for each OD pair, the number of ridesharing riders should be greater than or equal to the number of ridesharing drivers.

$$f_{p_3^{r^1s}} + f_{p_3^{r^0s}} \geq f_{p_2^{r^1s}}, \quad \forall p_3^{rs} \in P_3^{rs}, p_2^{r^0s} \in P_2^{r^0s}, r \in R, s \in S \tag{16}$$

where $f_{p_3^{r^1s}}$ is the travel flow on path p^{r^1s} between OD pair r^1s in the extended network, i.e., the number of car owners travel as ridesharing riders on path p^{rs} between OD pair rs in the original network. Similarly, $f_{p_3^{r^0s}}$ represents the number of non-car owners travel as ridesharing riders on path p^{rs} between OD pair rs, and $f_{p_2^{r^1s}}$ represents the number of ridesharing drivers on path p^{rs} between OD pair rs.

Upper bound constraint: Meanwhile, there is a certain capacity Cap for each ridesharing vehicle. Cap is the upper bound of the number of riders that each ridesharing vehicle can take or each ridesharing driver can pick up. Therefore, although each ridesharing driver is allowed to pick up multiple riders, for each OD pair, the total number of ridesharing riders should not exceed the capacity of all ridesharing vehicles. This relationship can be represented by the following inequality:

$$f_{p_3^{r^1s}} + f_{p_3^{r^0s}} \leq Cap \cdot f_{p_2^{r^1s}}, \quad \forall p_3^{rs} \in P_3^{rs}, p_2^{r^0s} \in P_2^{r^0s}, r \in R, s \in S \tag{17}$$

Definition 1 (*Saturated conditions*). We define the path p^{rs} between OD pair rs in the original network is under saturated conditions, if the lower bound constraint or the upper bound constraint holds with equality, i.e,. $f_{p_3^{r^1s}} + f_{p_3^{r^0s}} = f_{p_2^{r^1s}}$ or $f_{p_3^{r^1s}} + f_{p_3^{r^0s}} = Cap \cdot f_{p_2^{r^1s}}$. The former indicates each ridesharing driver can only pick up one ridesharing rider. The latter indicates the number of ridesharing riders reaches the capacity that all ridesharing vehicles can take.

The above inequalities in Eqs.(16-17) are two side constraints that are introduced into the multi-user stochastic traffic assignment problem due to the inherent relationship between the number of ridesharing drivers and the number of ridesharing riders (Larsson and Patriksson, 1999). As described above, they have well-defined physical meanings.

Let κ be the set of feasible path flow $f_{p_k^{rs}}$ (i.e., feasible mode-specific flow and path flow for car owners and non-car owners) defined by the above constraints,

$$\kappa = \left\{ \mathbf{f} | f_{p_k^{r^1s}}, f_{p_k^{r^0s}} \text{ satisfies constraints in Eq.}(12-17) \right\}. \tag{18}$$

where $\mathbf{f}$ is the column vector of path flow $f_{p_k^{rs}}$, it has $\mathbf{f} = \left\{ f_{p_k^{r^1 s}}, f_{p_k^{r^0 s}}, \ \forall r^1 \in R^1, r^0 \in R^0, s \in S, k \in K \right\}$.

Variable preprocessing. Note that based on physical meanings of the lower bound constraint in Eq.(16) and the upper bound constraint in Eq.(17), as the average occupancy rate of each ridesharing vehicle (i.e., the average number of riders that each ridesharing driver picks up) on path p^{rs} between OD pair rs, $v_{p^{rs}}$ should satisfy $v_{p^{rs}} \geq 1$ and $v_{p^{rs}} \leq Cap$. However, as calculated in Eq.(8), $v_{p^{rs}} = \frac{f_{p_3^{r^1 s}} + f_{p_3^{r^0 s}}}{f_{p_2^{r^1 s}}}$. It will cause $v_{p^{rs}} \to +\infty$ when the number of travelers on path $p_2^{r^1 s}$ approaches zero (i.e., $f_{p_2^{r^1 s}} \to 0$). To avoid this mistake, the average occupancy rate $v_{p^{rs}}$ can be calculated by solving a linear complementarity problem in Eqs.(19-20) instead of the calculation in Eq.(8).

$[LNP - v_{p^{rs}}]$: The linear complementarity problem is to find $v_{p^{rs}} \in \mathbb{R}$ such that:

$$0 \leq f_{p_2^{r^1 s}} \cdot v_{p^{rs}} - \left(f_{p_3^{r^1 s}} + f_{p_3^{r^0 s}} \right) + \lambda_{v-}^{p^{rs}} \quad \perp \quad v_{p^{rs}} - 1 \geq 0 \tag{19}$$

$$0 \leq \lambda_{v-}^{p^{rs}} \quad \perp \quad Cap - v_{p^{rs}} \geq 0 \tag{20}$$

where $\lambda_{v-}^{p^{rs}}$ denotes the Lagrange multiplier corresponding to the constraint $v_{p^{rs}} \leq Cap$.

Proposition 1 (Equivalence). Solving the linear complementarity problem $[LNP - v_{p^{rs}}]$ is equivalent to the calculation of $v_{p^{rs}}$ according to Eq.(8).

Proof. $v_{p^{rs}}$ can be regarded as the optimal solution of the following quadratic program (Di et al., 2018):

$$v_{p^{rs}} = arg \min_{v_{p^{rs}} \in [1, Cap]} \frac{f_{p_2^{r^1 s}}}{2} \cdot {v_{p^{rs}}}^2 - \left(f_{p_3^{r^1 s}} + f_{p_3^{r^0 s}} \right) \cdot v_{p^{rs}} \tag{21}$$

Namely, the quadratic program is

$$\min_{\tau} \quad \frac{f_{p_2^{r^1 s}}}{2} \cdot {v_{p^{rs}}}^2 - \left(f_{p_3^{r^1 s}} + f_{p_3^{r^0 s}} \right) \cdot v_{p^{rs}} \tag{22}$$

s.t.

$$v_{p^{rs}} \geq 1 \tag{23}$$

$$v_{p^{rs}} \leq Cap \tag{24}$$

The optimal solution $v_{p^{rs}}$ should satisfy the first-order necessary optimality conditions (i.e., KKT conditions) of the quadratic program:

$$f_{p_2^{r^1 s}} \cdot v_{p^{rs}} - \left(f_{p_3^{r^1 s}} + f_{p_3^{r^0 s}} \right) - \lambda_{v+}^{p^{rs}} + \lambda_{v-}^{p^{rs}} = 0 \tag{25}$$

$$0 \leq \lambda_{v+}^{p^{rs}} \quad \perp \quad v_{p^{rs}} - 1 \geq 0 \tag{26}$$

$$0 \leq \lambda_{v-}^{p^{rs}} \quad \perp \quad Cap - v_{p^{rs}} \geq 0 \tag{27}$$

where $\lambda_{v+}^{p^{rs}}$ and $\lambda_{v-}^{p^{rs}}$ denote the Lagrange multipliers corresponding to the constraint $v_{p^{rs}} \geq 1$ and $v_{p^{rs}} \leq Cap$ respectively.

Then, taking $\lambda_{v+}^{p^{rs}} = f_{p_2^{r^1s}} \cdot v_{p^{rs}} - \left(f_{p_3^{r^1s}} + f_{p_3^{r^0s}}\right) + \lambda_{v-}^{p^{rs}}$ into Eq.(26), we can derive the linear complementarity conditions of $[LNP - v_{p^{rs}}]$ as shown in Eqs.(19-20). Therefore, solving the linear complementarity problem $[LNP - v_{p^{rs}}]$ is equivalent to the calculation of $v_{p^{rs}}$ in Eq.(8). □

(3) Generalized path travel cost in the extended network

Due to the existence of inequality constraints on the path flow in Eqs.(16-17), the equivalent route choice problem in the extended network is a side constrained traffic assignment problem. To formulate the side constrained traffic assignment problem, we define a generalized path travel cost by introducing the following Lagrange multipliers.

$\lambda_+^{p^{rs}}$ and $\lambda_-^{p^{rs}}$ are two Lagrange multipliers corresponding to the lower bound constraint in Eq.(16) and the upper bound constraint in Eq.(17) on path p^{rs} between OD pair rs, respectively. They satisfy the following complementarity conditions:

$$0 \le \lambda_+^{p^{rs}} \quad \perp \quad f_{p_3^{r^1s}} + f_{p_3^{r^0s}} - f_{p_2^{r^1s}} \ge 0, \ \ \forall p^{rs} \in P^{rs}, r \in R, s \in S \tag{28}$$

$$0 \le \lambda_-^{p^{rs}} \quad \perp \quad Cap \cdot f_{p_2^{r^1s}} - f_{p_3^{r^1s}} - f_{p_3^{r^0s}} \ge 0, \ \ \forall p^{rs} \in P^{rs}, r \in R, s \in S \tag{29}$$

Definition 2 (*Generalized path travel cost*). For each travel path between OD pair r^1s and r^0s, the generalized path travel cost $\tilde{C}_{p_k^{rs}}$ is consist of the path travel cost $C_{p_k^{rs}}$ and a linear function of the Lagrange multipliers $\lambda_+^{p^{rs}}$ and $\lambda_-^{p^{rs}}$ (Larsson and Patriksson, 1999) as follows:

Generalized travel cost of path $p_1^{r^1s}$ (Solo drivers):

$$\tilde{C}_{p_1^{r^1s}} = C_{p_1^{r^1s}}, \ \ \forall p_1^{r^1s} \in P_1^{r^1s}, r^1 \in R^1, s \in S \tag{30}$$

Generalized travel cost of path $p_2^{r^1s}$ (Ridesharing drivers):

$$\tilde{C}_{p_2^{r^1s}} = C_{p_2^{r^1s}} + \lambda_+^{p^{rs}} - Cap \cdot \lambda_-^{p^{rs}}, \ \ \forall p_2^{r^1s} \in P_2^{r^1s}, r^1 \in R^1, s \in S \tag{31}$$

Generalized travel cost of path $p_3^{r^1s}$ (Ridesharing riders for car owners):

$$\tilde{C}_{p_3^{r^1s}} = C_{p_3^{r^1s}} - \lambda_+^{p^{rs}} + \lambda_-^{p^{rs}}, \ \ \forall p_3^{r^1s} \in P_3^{r^1s}, r^1 \in R^1, s \in S \tag{32}$$

Generalized travel cost of path $p_3^{r^0s}$ (Ridesharing riders for non-car owners):

$$\tilde{C}_{p_3^{r^0s}} = C_{p_3^{r^0s}} - \lambda_+^{p^{rs}} + \lambda_-^{p^{rs}}, \quad \forall p_3^{r^0s} \in P_3^{r^0s}, r^0 \in R^0, s \in S \tag{33}$$

Generalized travel cost of path $p_4^{r^0s}$ (Public transit riders):

$$\tilde{C}_{p_4^{r^0s}} = C_{p_4^{r^0s}}, \ \ \forall p_4^{r^0s} \in P_4^{r^0s}, r^0 \in R^0, s \in S \tag{34}$$

Lagrange multipliers for path flow constraints can be given interesting interpretations. According to Eqs.(28-29), $\lambda_+^{p^{rs}}$ and $\lambda_-^{p^{rs}}$ are not positive at the same time, i.e., $\lambda_+^{p^{rs}} > 0, \lambda_-^{p^{rs}} = 0$ or $\lambda_+^{p^{rs}} = 0, \lambda_-^{p^{rs}} > 0$. Thus, as for the second item and the third item on the right side of Eqs.(31-32), at most one item is positive.

Based on the definition of generalized path travel cost in Eqs.(32-33), $\lambda_+^{p^{rs}}$ can be regard as a ridesharing payment reduction for each ridesharing rider on path p^{rs} between OD pair rs.

Moreover, $\lambda_+^{p^{rs}} > 0$ can derive $f_{p_3^{r1_s}} + f_{p_3^{r0_s}} = f_{p_2^{r1_s}}$ which means the number of ridesharing drivers equals to the number of ridesharing riders on path p^{rs} between OD pair rs. For the path p^{rs} between OD pair rs, each ridesharing driver only picks up one ridesharing rider. Therefore, according to the definition of generalized path travel cost in Eqs.(31), $\lambda_+^{p^{rs}}$ can also be regarded as a ridesharing compensation reduction for each ridesharing driver on path p^{rs} between OD pair rs.

Similarly, based on the definition of generalized path travel cost in Eqs.(32-33), $\lambda_-^{p^{rs}}$ can be regard as a ridesharing payment increment for each ridesharing rider on path p^{rs} between OD pair rs. Moreover, $\lambda_-^{p^{rs}} > 0$ can derive $f_{p_3^{r1_s}} + f_{p_3^{r0_s}} = Cap \cdot f_{p_2^{r1_s}}$ which means, for each ridesharing driver on path p^{rs} between OD pair rs, the number of ridesharing riders he/she picked up has reached the capacity of the ridesharing vehicle Cap. Therefore, $Cap \cdot \lambda_-^{p^{rs}}$ can also be regard as the ridesharing compensation increment for each ridesharing driver on path p^{rs} between OD pair rs.

Note (*Actual ridesharing payment/compensation, physical meaning of the generalized path travel cost*). τ^{rs} is the basic ridesharing payment/compensation determined according to a pre-specified pricing scheme, while $\lambda_+^{p^{rs}}$ and $\lambda_-^{p^{rs}}$ are the ridesharing payment/compensation reduction and increment determined by the ridesharing market according to the relationship between ridesharing supply (i.e., ridesharing drivers) and ridesharing demand (i.e., ridesharing riders) as illustrated in Eqs.(28-29). Moreover, $\lambda_+^{p^{rs}}$ and $\lambda_-^{p^{rs}}$ are not positive at the same time. Thus, based on the physical meaning of Lagrange multipliers for path flow constraints as described above, the actual ridesharing payment for each rider on path p^{rs} between OD pair rs is $\tau^{rs} - \lambda_+^{p^{rs}} + \lambda_-^{p^{rs}}$, while the actual ridesharing compensation for each driver on path p^{rs} between OD pair rs is $v^{p^{rs}}\tau^{rs} - \lambda_+^{p^{rs}} + Cap \cdot \lambda_-^{p^{rs}}$. From the perspective of travelers, the generalized travel cost in **Definition 2** is the actual travel cost for each travel mode in the urban traffic system with the introduction of ridesharing programs.

By adjusting the generalized travel cost of ridesharing participants (i.e., ridesharing drivers and ridesharing riders), the ridesharing payment reduction or increment restrains the traffic flow on each path (i.e., the number of ridesharing drivers and ridesharing riders) to a predetermined relationship in Eqs.(16-17).

3.2 Stochastic traffic assignment model with side constraints and multi-user classes

By modifying the path travel cost $\left\{C_{p_k^{rs}},\ \forall p_k^{rs} \in P_k^{rs}, r \in R, s \in S, k \in K\right\}$ as the generalized path travel cost $\left\{\tilde{C}_{p_k^{rs}},\ \forall p_k^{rs} \in P_k^{rs}, r \in R, s \in S, k \in K\right\}$, we firstly define the logit-based generalized SUE in terms of path flow $\mathbf{f}$. Namely, based on the well-defined generalized path travel cost, conditions that path flow $\mathbf{f}^* \in \kappa$ is referred to a logit-based generalized SUE in Section 3.1 are proposed. Then, the mixed complementarity problem formulation of the stochastic traffic assignment problem is proposed and solved to obtain the stochastic equilibrium path flow $\mathbf{f}^*$.

3.2.1 Logit-based generalized stochastic user equilibrium

Due to the limited perceived ability, travelers cannot perceive the actual travel cost of each mode choice exactly. Thus, there is always a stochastic error ϵ_k between the perceived generalized path travel cost and the actual generalized path travel cost for each traveler. Since the error terms associated with all paths are assumed to be identically distributed, ϵ_k can be replaced by ϵ, and the perceived generalized travel cost of path p_k^{rs} is $\tilde{C}_{p_k^{rs}} + \epsilon$. Accordingly, as rational travelers, they make route choice decisions in the extended network so as to minimize the expected value of the perceived generalized path travel cost. The logit-based stochastic route choice model derived from the Gumbel error distribution is adopted to formulate the route choice behavior in the extended network.

In the extended network, $\mathbf{f}$ is the vector of path flows as defined in Eq.(18). $\boldsymbol{\lambda}$ is the vector of Lagrangian multipliers in Eqs.(28-29). $\mathbf{C}(\mathbf{f})$ is the vector of path travel costs in Eqs.(6,7,9-11) which is a function of the vector of path travel flow $\mathbf{f}$. $\tilde{\mathbf{C}}(\mathbf{f}, \boldsymbol{\lambda})$ denotes the vector of generalized path travel costs in Eqs.(30-34) which is a function of the vector of path travel flow $\mathbf{f}$ and the vector of Lagrangian multipliers $\boldsymbol{\lambda}$. Specifically, $\mathbf{f}$, $\boldsymbol{\lambda}$, $\mathbf{C}(\mathbf{f})$, and $\tilde{\mathbf{C}}(\mathbf{f}, \boldsymbol{\lambda})$ are defined as follows:

$$\mathbf{f} = \left(f_{p_1^{r^1s}}, f_{p_2^{r^1s}}, f_{p_3^{r^1s}}, f_{p_3^{r^0s}}, f_{p_4^{r^0s}}, \cdots\right)^T,$$

$$\boldsymbol{\lambda} = \left(\lambda_+^{p^{rs}}, \lambda_-^{p^{rs}}, \cdots\right)^T,$$

$$\mathbf{C}(\mathbf{f}) = \left(C_{p_1^{r^1s}}(\mathbf{f}), C_{p_2^{r^1s}}(\mathbf{f}), C_{p_3^{r^1s}}(\mathbf{f}), C_{p_3^{r^0s}}(\mathbf{f}), C_{p_4^{r^0s}}(\mathbf{f}), \cdots\right)^T,$$

$$\tilde{\mathbf{C}}(\mathbf{f}, \boldsymbol{\lambda}) = \left(\tilde{C}_{p_1^{r^1s}}(\mathbf{f}, \boldsymbol{\lambda}), \tilde{C}_{p_2^{r^1s}}(\mathbf{f}, \boldsymbol{\lambda}), \tilde{C}_{p_3^{r^1s}}(\mathbf{f}, \boldsymbol{\lambda}), \tilde{C}_{p_3^{r^0s}}(\mathbf{f}, \boldsymbol{\lambda}), \tilde{C}_{p_4^{r^0s}}(\mathbf{f}, \boldsymbol{\lambda}), \cdots\right)^T.$$

Thus, the probability that path $p_k^{r^1s}$ chosen by car owners (i.e., $Pr_{p_k^{r^1s}}$) is calculated:

$$Pr_{p_k^{r^1s}}\left(\tilde{\mathbf{C}}(\mathbf{f}, \boldsymbol{\lambda})\right) = \frac{\exp\left(-\theta \tilde{C}_{p_k^{r^1s}}\right)}{\sum_{j \in K^1} \exp\left(-\theta \tilde{C}_{p_j^{r^1s}}\right)}, \quad \forall p_k^{r^1s} \in P_k^{r^1s}, r^1 \in R^1, s \in S, k \in K^1 \tag{35}$$

Similarly, the probability that path $p_k^{r^0s}$ chosen by non-car owners (i.e., $Pr_{p_k^{r^0s}}$) is:

$$Pr_{p_k^{r^0s}}\left(\tilde{\mathbf{C}}(\mathbf{f}, \boldsymbol{\lambda})\right) = \frac{\exp\left(-\theta \tilde{C}_{p_k^{r^0s}}\right)}{\sum_{j \in K^0} \exp\left(-\theta \tilde{C}_{p_j^{r^0s}}\right)}, \quad \forall p_k^{r^0s} \in P_k^{r^0s}, r^0 \in R^0, s \in S, k \in K^0 \tag{36}$$

where θ is a parameter that scales the perceptual error on the actual generalized path travel cost. The higher the value of θ, the smaller the perception variation will be. If $\theta = +\infty$, all travelers will choose the route whose generalized path travel cost is the smallest. Namely, it indicates all travelers know urban traffic conditions very well which are the preconditions of user equilibrium. However, if $\theta = 0$, travelers will choose each path with equal probability.

Travelers in the extended network choose travel paths according to the probability in Eqs.(35-36). Eventually, all travelers belong to each category (i.e., car owners, non-car owners) can make the best route choice in the extended network (i.e., the best mode choice and route choice in the

original network) to minimize their individual expected value of the perceived generalized path travel cost, which can be described by the multi-class multi-criteria generalized SUE state. At the multi-class multi-criteria generalized SUE, each category of travelers shares the same expected value of the perceived generalized path travel cost no matter which route they choose, nobody can reduce his/her expected value of the perceived generalized path travel cost by unilaterally changing routes.

Definition 3 (*Generalized stochastic user equilibrium conditions*). Under the steady-state presumption (Larsson and Patriksson, 1999), the logit-based generalized stochastic user equilibrium conditions with side constraints and multi-user classes in the path-based forms can be defined as follows. Let $\mathbf{f}$ denote a set of path flows that satisfy constraints in Eqs.(12-17). $\mathbf{f}$ is referred to a generalized stochastic user equilibrium path flow pattern for the stochastic traffic assignment problem with side constraints and multi-user classes if and only if there is a set of $\boldsymbol{\lambda}$ satisfying constraints in Eqs.(28-29), such that:

$$f_{p_k^{r^1 s}} = q^{r^1 s} \cdot Pr_{p_k^{r^1 s}}\left(\tilde{\mathbf{C}}\left(\mathbf{f}, \boldsymbol{\lambda}\right)\right), \quad \forall p_k^{r^1 s} \in P_k^{r^1 s}, r^1 \in R^1, s \in S, k \in K^1 \tag{37}$$

$$f_{p_k^{r^0 s}} = q^{r^0 s} \cdot Pr_{p_k^{r^0 s}}\left(\tilde{\mathbf{C}}\left(\mathbf{f}, \boldsymbol{\lambda}\right)\right), \quad \forall p_k^{r^0 s} \in P_k^{r^0 s}, r^0 \in R^0, s \in S, k \in K^0 \tag{38}$$

where $q^{r^1 s}, q^{r^0 s}$ are the travel demand of OD pair $r^1 s$ and $r^0 s$ which are exogenously given. $\tilde{\mathbf{C}}\left(\mathbf{f}, \boldsymbol{\lambda}\right)$ is a function of the path travel cost $\mathbf{C}\left(\mathbf{f}\right)$ and Lagrange multipliers $\boldsymbol{\lambda}$, i.e., $\tilde{\mathbf{C}}\left(\mathbf{f}, \boldsymbol{\lambda}\right) = \mathbf{C}\left(\mathbf{f}\right) + \boldsymbol{\Lambda}\boldsymbol{\lambda}$. $\boldsymbol{\Lambda}$ is the coefficient matrix of Lagrange multipliers as shown in **Definition 2**.

Proposition 2 (*Actual ridesharing payment/compensation under SUE with saturated conditions*). When the urban traffic system reaches SUE $\mathbf{f}^*$ and path p^{rs} reaches saturated conditions, adjusting the basic ridesharing payment/compensation τ^{rs} within a certain range (i.e., $[\tau^{rs*} - \max_{p^{rs} \in P^{rs}} \lambda_+^{p^{rs}*}, +\infty)$ or $[0, \tau^{rs*} + \min_{p^{rs} \in P^{rs}} \lambda_-^{p^{rs}*}]$) will not change the actual ridesharing payment for each rider and the actual ridesharing compensation for each driver.

Proof. If the urban traffic system reaches SUE $\mathbf{f}^*$ and $f^*_{p_3^{r^1 s}} + f^*_{p_3^{r^0 s}} = f^*_{p_2^{r^1 s}}$, the actual ridesharing payment for each rider and the actual ridesharing compensation for each driver on path p_k^{rs} are the same and equal to $\tau^{rs*} - \lambda_+^{p^{rs}*}$. If the urban traffic system reaches SUE $\mathbf{f}^*$ and $f^*_{p_3^{r^1 s}} + f^*_{p_3^{r^0 s}} = Cap \cdot f^*_{p_2^{r^1 s}}$, the actual ridesharing payment for each rider and the actual ridesharing compensation for each driver on path p_k^{rs} are equal to $\tau^{rs*} + \lambda_-^{p^{rs}*}$ and $Cap \cdot \left(\tau^{rs*} + \lambda_-^{p^{rs}*}\right)$ respectively. It can be further demonstrated that for two scenarios discussed above, the travel flow on path p_k^{rs} between OD pair rs is strictly monotone with the actual ridesharing payment/compensation according to Eqs.(30-34, 37-38).

Therefore, when we adjust the basic ridesharing payment/compensation τ^{rs} within the range of $[\tau^{rs*} - \max_{p^{rs} \in P^{rs}} \lambda_+^{p^{rs}*}, +\infty)$ in the former scenario or $[0, \tau^{rs*} + \min_{p^{rs} \in P^{rs}} \lambda_-^{p^{rs}*}]$ in the latter scenario, the ridesharing market can still change the value of ridesharing payment/compensation reduction and increment (i.e., $\lambda_+^{p^{rs}}, \lambda_-^{p^{rs}}$) to guarantee the urban traffic system stays at SUE $\mathbf{f}^*$ under the premise of $\lambda_+^{p^{rs}} \geq 0, \lambda_-^{p^{rs}} \geq 0$. Meanwhile, the actual ridesharing payment for each rider and the actual ridesharing compensation for each driver keep unchanged.

3.2.2 Mixed complementarity problem formulation

According to Eqs.(6-11), we can know the travel cost function is inseparable and asymmetric. Travelers are heterogeneous in terms of car ownership and VOT. Moreover, there are several side constraints on the path flow as shown in Eqs.(16-17). Thus, the route choice at stochastic user equilibrium state in the extended network is an asymmetric stochastic traffic equilibrium problem with side constraints and multi-user classes. It is well-known that there is no equivalent mathematical programming due to the complexity of the travel cost function. Instead, in this subsection, this generalized SUE problem with ridesharing services is formulated as a variational inequality problem firstly. Then, to overcome the challenging numerical computation, we further reformulate it as an equivalent mixed complementarity problem that can be efficiently solved by the optimization solver.

Specifically, the path-based generalized SUE is formulated as a variational inequality problem below.

Definition 4. Given the set of feasible path flows κ which is a subset of the Euclidean $\left(|K^1|+|K^0|\right)|R||S|$-dimensional space $\mathbb{R}^{\left(|K^1|+|K^0|\right)|R||S|}$ and a mapping $\mathbf{\Phi}: \kappa \rightarrow \mathbb{R}^{\left(|K^1|+|K^0|\right)|R||S|}$, $\mathbf{\Phi}(\mathbf{f}) = \mathbf{C}(\mathbf{f}) + \frac{1}{\theta}(1+\ln \mathbf{f})$. The variational inequality, denoted by $VI(\mathbf{\Phi}, \kappa)$, is to find a vector $\mathbf{f}^* \in \kappa$ such that:

$$\mathbf{\Phi}(\mathbf{f}^*)^T(\mathbf{f}-\mathbf{f}^*) \geq 0, \quad \forall \mathbf{f} \in \kappa \tag{39}$$

where κ is the feasible solution space of path flow $\mathbf{f}$ as defined in Eq.(18).

Theorem 1. A path flow pattern $\mathbf{f}^* \in \kappa$ is in a logit-based generalized SUE as defined in **Definition 3** if and only if it solves the variational inequality problem $VI(\mathbf{\Phi}, \kappa)$ in **Definition 4**.

Proof. If $\mathbf{f}^*$ is a solution of $VI(\mathbf{\Phi}, \kappa)$, we have

$$\mathbf{\Phi}(\mathbf{f}^*)^T\mathbf{f} \geq \mathbf{\Phi}(\mathbf{f}^*)^T\mathbf{f}^*, \quad \forall \mathbf{f} \in \kappa \tag{40}$$

This implies $\mathbf{f}^*$ is the solution of the following linear program:

$$\min_{\mathbf{f}\in\kappa} \quad \mathbf{\Phi}(\mathbf{f}^*)^T\mathbf{f} \tag{41}$$

By using the primal-dual optimality conditions, the sufficient and necessary conditions for $\mathbf{f}^*$ to be the solution of linear program are:

$$f^*_{p_1^{r^1s}}\left(C_{p_1^{r^1s}}(\mathbf{f}^*) + \frac{1}{\theta}(1+\ln f^*_{p_1^{r^1s}}) - \mu^{r^1s}\right) = 0, \quad \forall p_1^{r^1s} \in P_1^{r^1s}, r^1 \in R^1, s \in S \tag{42}$$

$$C_{p_1^{r^1s}}(\mathbf{f}^*) + \frac{1}{\theta}(1+\ln f^*_{p_k^{r^1}}) - \mu^{r^1s} \geq 0, \quad \forall p_1^{r^1s} \in P_1^{r^1s}, r^1 \in R^1, s \in S \tag{43}$$

$$f^*_{p_2^{r^1s}}\left(C_{p_2^{r^1s}}(\mathbf{f}^*) + \frac{1}{\theta}(1+\ln f^*_{p_2^{r^1s}}) + \lambda_+^{p^{rs}} - Cap\cdot\lambda_-^{p^{rs}} - \mu^{r^1s}\right) = 0, \quad \forall p^{rs} \in P^{rs}, r \in R, s \in S \tag{44}$$

$$C_{p_2^{r^1s}}(\mathbf{f}^*) + \frac{1}{\theta}(1+\ln f^*_{p_2^{r^1s}}) + \lambda_+^{p^{rs}} - Cap\cdot\lambda_-^{p^{rs}} - \mu^{r^1s} \geq 0, \quad \forall p^{rs} \in P^{rs}, r \in R, s \in S \tag{45}$$

$$f^*_{p_3^{r^1s}}\left(C_{p_3^{r^1s}}(\mathbf{f}^*) + \frac{1}{\theta}(1+\ln f^*_{p_3^{r^1s}}) - \lambda_+^{p^{rs}} + \lambda_-^{p^{rs}} - \mu^{r^1s}\right) = 0, \quad \forall p^{rs} \in P^{rs}, r \in R, s \in S \tag{46}$$

$$C_{p_3^{r^1s}}(\mathbf{f}^*) + \frac{1}{\theta}(1+\ln f^*_{p_3^{r^1s}}) - \lambda_+^{p^{rs}} + \lambda_-^{p^{rs}} - \mu^{r^1s} \geq 0, \quad \forall p^{rs} \in P^{rs}, r \in R, s \in S \tag{47}$$

$$f^*_{p_3^{r^0s}}\left(C_{p_3^{r^0s}}(\mathbf{f}^*)+\frac{1}{\theta}(1+\ln f^*_{p_3^{r^0s}})-\lambda_+^{p^{rs}}+\lambda_-^{p^{rs}}-\mu^{r^0s}\right)=0,\ \ \forall p^{rs}\in P^{rs}, r\in R, s\in S \tag{48}$$

$$C_{p_3^{r^0s}}(\mathbf{f}^*)+\frac{1}{\theta}(1+\ln f^*_{p_3^{r^0s}})-\lambda_+^{p^{rs}}+\lambda_-^{p^{rs}}-\mu^{r^0s}\geq 0,\ \ \forall p^{rs}\in P^{rs}, r\in R, s\in S \tag{49}$$

$$f^*_{p_4^{r^0s}}\left(C_{p_4^{r^0s}}(\mathbf{f}^*)+\frac{1}{\theta}(1+\ln f^*_{p_4^{r^0s}})-\mu^{r^0s}\right)=0,\ \ \forall p_4^{r^0s}\in P_4^{r^0s}, r^0\in R^0, s\in S \tag{50}$$

$$C_{p_4^{r^0s}}(\mathbf{f}^*)+\frac{1}{\theta}(1+\ln f^*_{p_4^{r^0s}})-\mu^{r^0s}\geq 0,\ \ \forall p_4^{r^0s}\in P_4^{r^0s}, r^0\in R^0, s\in S \tag{51}$$

$$\text{Demand constraints: } Eqs.(12-13) \tag{52}$$

$$\text{Lagrange multipliers and bound constraints: } Eqs.(28-29) \tag{53}$$

$$\text{Non-negative constraints: } \mathbf{f}^*\geq \mathbf{0} \tag{54}$$

where μ^{r^1s}, μ^{r^0s} are two multipliers associated with demand constraints in Eq.(12) and Eq.(13). For every effective path $p_k^{r^1s}, p_k^{r^0s}$, there should be $f^*_{p_k^{r^1s}}>0, f^*_{p_k^{r^0s}}>0$. Thus, Eqs.(43,45,47,49,51) hold for any OD pair with equality. We can obtain

$$f^*_{p_1^{r^1s}}=\exp\left(-\theta C_{p_1^{r^1s}}(\mathbf{f}^*)+\theta\mu^{r^1s}-1\right),\ \ \forall p_1^{r^1s}\in P_1^{r^1s}, r^1\in R^1, s\in S \tag{55}$$

$$f^*_{p_2^{r^1s}}=\exp\left(-\theta C_{p_2^{r^1s}}(\mathbf{f}^*)-\theta\left(\lambda_+^{p^{rs}}-Cap\cdot\lambda_-^{p^{rs}}\right)+\theta\mu^{r^1s}-1\right),\ \ \forall p^{rs}\in P^{rs}, r\in R, s\in S \tag{56}$$

$$f^*_{p_3^{r^1s}}=\exp\left(-\theta C_{p_3^{r^1s}}(\mathbf{f}^*)+\theta\left(\lambda_+^{p^{rs}}-\lambda_-^{p^{rs}}\right)+\theta\mu^{r^1s}-1\right),\ \ \forall p^{rs}\in P^{rs}, r\in R, s\in S \tag{57}$$

$$f^*_{p_3^{r^0s}}=\exp\left(-\theta C_{p_3^{r^0s}}(\mathbf{f}^*)+\theta\left(\lambda_+^{p^{rs}}-\lambda_-^{p^{rs}}\right)+\theta\mu^{r^0s}-1\right),\ \ \forall p^{rs}\in P^{rs}, r\in R, s\in S \tag{58}$$

$$f^*_{p_4^{r^0s}}=\exp\left(-\theta C_{p_4^{r^0s}}(\mathbf{f}^*)+\theta\mu^{r^0s}-1\right),\ \ \forall p_4^{r^0s}\in P_4^{r^0s}, r^0\in R^0, s\in S \tag{59}$$

Combining the demand constraints in Eq.(12) and Eq.(13), we can derive the logit-based route choice model in Eq.(35) and Eq.(36) respectively. It implies that the variational inequality problem $VI(\mathbf{\Phi},\kappa)$ is equivalent to the generalized SUE conditions in **Definition 3**. The proof is complete.□

For efficient computation, a path-based mixed complementarity problem $MiCP(\mathbf{F})$ is further established to model the logit-based generalized SUE problem. Because the feasible solution space κ is a polyhedron, the equivalency between the variational inequality problem $VI(\mathbf{\Phi},\kappa)$ and the mixed complementarity problem $MiCP(\mathbf{F})$ can be derived according to Proposition 2.2 in Harker et al. (1990) or Proposition 1.2.1 in Facchinei et al. (2007). Let $\boldsymbol{\mu}$ represent the vector of multipliers of demand constraints, i.e., $\boldsymbol{\mu}=\left(\mu^{r^1s},\mu^{r^0s},\cdots\right)^T$. The mixed complementarity problem $MiCP(\mathbf{F})$ is defined in **Definition 5**.

Definition 5. Given a continuous mapping $\mathbf{F}:\mathbb{R}^{\left(|K^1|+|K^0|\right)|R||S|}\rightarrow\mathbb{R}^{\left(|K^1|+|K^0|\right)|R||S|}$. The mixed complementarity problem, denoted by $MiCP(\mathbf{F})$, is to find a vector $(\mathbf{f},\boldsymbol{\lambda},\boldsymbol{\mu})$ such that:

$$0\leq f_{p_1^{r^1s}}\ \ \perp\ \ C_{p_1^{r^1s}}(\mathbf{f})+\frac{1}{\theta}(1+\ln f_{p_1^{r^1s}})-\mu^{r^1s}\geq 0,\ \ \forall p_1^{r^1s}\in P_1^{r^1s}, r^1\in R^1, s\in S \tag{60}$$

$$0\leq f_{p_2^{r^1s}}\ \ \perp\ \ C_{p_2^{r^1s}}(\mathbf{f})+\frac{1}{\theta}(1+\ln f_{p_2^{r^1s}})+\lambda_+^{p^{rs}}-Cap\cdot\lambda_-^{p^{rs}}-\mu^{r^1s}\geq 0,\ \ \forall p^{rs}\in P^{rs}, r\in R, s\in S \tag{61}$$

$$0\leq f_{p_3^{r^1s}}\ \ \perp\ \ C_{p_3^{r^1s}}(\mathbf{f})+\frac{1}{\theta}(1+\ln f_{p_3^{r^1s}})-\lambda_+^{p^{rs}}+\lambda_-^{p^{rs}}-\mu^{r^1s}\geq 0,\ \ \forall p^{rs}\in P^{rs}, r\in R, s\in S \tag{62}$$

$$0 \le f_{p_3^{r^0 s}} \perp C_{p_3^{r^0 s}}(\mathbf{f}) + \frac{1}{\theta}(1 + \ln f_{p_3^{r^0 s}}) - \lambda_+^{p^{rs}} + \lambda_-^{p^{rs}} - \mu^{r^0 s} \ge 0, \ \forall p^{rs} \in P^{rs}, r \in R, s \in S \quad (63)$$

$$0 \le f_{p_4^{r^0 s}} \perp C_{p_4^{r^0 s}}(\mathbf{f}) + \frac{1}{\theta}(1 + \ln f_{p_4^{r^0 s}}) - \mu^{r^0 s} \ge 0, \ \forall p_4^{r^0 s} \in P_4^{r^0 s}, r^0 \in R^0, s \in S \quad (64)$$

$$0 \le \lambda_+^{p^{rs}} \perp f_{p_3^{r^1 s}} + f_{p_3^{r^0 s}} - f_{p_2^{r^1 s}} \ge 0, \ \forall p^{rs} \in P^{rs}, r \in R, s \in S \quad (65)$$

$$0 \le \lambda_-^{p^{rs}} \perp Cap \cdot f_{p_2^{r^1 s}} - f_{p_3^{r^1 s}} - f_{P_3^{r^0 s}} \ge 0, \ \forall p^{rs} \in P^{rs}, r \in R, s \in S \quad (66)$$

$$0 \le f_{p_2^{r^1 s}} \cdot v_{p^{rs}} - \left(f_{p_3^{r^1 s}} + f_{p_3^{r^0 s}}\right) + \lambda_{v-}^{p^{rs}} \perp v_{p^{rs}} - 1 \ge 0, \ \forall p^{rs} \in P^{rs}, r \in R, s \in S \quad (67)$$

$$0 \le \lambda_{v-}^{p^{rs}} \perp Cap - v_{p^{rs}} \ge 0, \ \forall p^{rs} \in P^{rs}, r \in R, s \in S \quad (68)$$

$$\mu^{r^1 s} \text{ free} \perp \sum_{k \in K^1} \sum_{p_k^{r^1} \in P_k^{r^1}} f_{p_k^{r^1}} - q^{r^1 s} = 0, \ \forall r^1 \in R^1, s \in S \quad (69)$$

$$\mu^{r^0 s} \text{ free} \perp \sum_{k \in K^0} \sum_{p_k^{r^0} \in P_k^{r^0}} f_{p_k^{r^0}} - q^{r^0 s} = 0, \ \forall r^0 \in R^0, s \in S \quad (70)$$

where Eqs.(60-64) indicate the SUE conditions for the extended network. Eqs.(65-66) represent the lower bound constraint and the upper bound constraint for the ridesharing system. Eqs.(67-68) define the average occupancy rate $v_{p^{rs}}$ of each ridesharing vehicle (i.e., the average number of riders that each ridesharing driver picks up) and make sure $v_{p^{rs}}$ satisfy the lower and upper bound constraints (i.e., $v_{p^{rs}} \ge 1$ and $v_{p^{rs}} \le Cap$). Eqs.(69-70) represent the path flow between each OD pair should satisfy the demand constraints in Eqs.(12-13).

3.3 Compensation optimization model

As described in section 3.1, each ridesharing rider should pay a sum of money to the ridesharing driver according to a pre-specified cost-sharing rule in the urban traffic system with the introduction of ridesharing programs. Thus, $\boldsymbol{\tau}$ denotes the ridesharing payment for ridesharing riders, while it is also the ridesharing compensation to ridesharing drivers for picking up one rider. We focus on how to determine the optimal compensation that each ridesharing driver should be received for picking up one rider in the ridesharing system from the perspective of traffic managers and policy-makers. Here, a compensation optimization model which is a bi-objective bi-level programming formulation is established to formulate and solve the decision-making problem of ridesharing compensation.

3.3.1 Bi-objective function

In the urban system with the introduction of ridesharing programs, traffic managers and policy-makers have two objectives from different perspectives when they make the decision of ridesharing compensation. As described in Section 2.2, they want to achieve two different goals at the same time. The detailed consideration of two different objective functions is listed as follows:

(1) Total generalized travel cost

Because as an emerging travel mode and a "real" sharing mobility service, ridesharing are widely recognized as a novel efficient method to relieve traffic congestions and reduce vehicular

air pollution emissions caused by the high private car ownership rate and the high percentage of people driving alone. For traffic managers and policy-makers, one consideration during decision-making of ridesharing compensation is the reduction of total generalized travel cost from the perspective of the efficiency of urban traffic systems. Accordingly, the first objective of this decision-making problem is the total generalized travel cost minimization which can be expressed as follows:

$$\min_{\boldsymbol{\tau}} \quad Z_1 = \sum_{r^1 \in R^1} \sum_{s \in S} \sum_{k \in K^1} \sum_{p_k^{r^1 s} \in P_k^{r^1 s}} f_{p_k^{r^1 s}} \tilde{C}_{p_k^{r^1 s}} \left(\mathbf{f}, \boldsymbol{\lambda}, \tau^{rs}\right) + \sum_{r^0 \in R^0} \sum_{s \in S} \sum_{k \in K^0} \sum_{p_k^{r^0 s} \in P_k^{r^0 s}} f_{p_k^{r^0 s}} \tilde{C}_{p_k^{r^0 s}} \left(\mathbf{f}, \boldsymbol{\lambda}, \tau^{rs}\right) \quad (71)$$

where Z_1 is the total generalized travel cost. It equals to the sum of the generalized travel cost of all travelers. $\boldsymbol{\tau}$ is the vector of ridesharing compensations, i.e., $\boldsymbol{\tau} = \{\tau^{rs},\ \forall r \in R, s \in S\}$. Note that because τ^{rs} is a variable rather than a constant in this subsection, The generalized path travel cost $\tilde{C}_{p_k^{r^1 s}} \left(\mathbf{f}, \boldsymbol{\lambda}, \tau^{rs}\right)$ is a function of the vector of path flow $\mathbf{f}$, the vector of Lagrange multipliers $\boldsymbol{\lambda}$, and the ridesharing compensation τ^{rs} as shown in Eqs.(6-11), which is different from $\tilde{C}_{p_k^{r^1 s}} \left(\mathbf{f}, \boldsymbol{\lambda}\right)$ in Section 3.1 and Section 3.2.

(2) Vehicular air pollution emissions

For traffic managers and policy-makers, another consideration during the decision-making of ridesharing compensation is the reduction of vehicular air pollution emissions since ridesharing is a sustainable travel mode. According to Li et al. (2016), Yin and Lawphongpanich (2006), the amount of air pollution emissions of a single vehicle on road a in the original network can be calculated as follows:

$$e_a = \varepsilon_1 t_a \left(x_a\right) \exp\left(\varepsilon_2 \frac{l_a}{t_a \left(x_a\right)}\right) \quad (72)$$

where e_a is air pollution emissions of a single vehicle on road a, measured in grams per vehicle. l_a is the length of road a (in kilometers). $t_a \left(x_a\right)$ is the travel time on road a (in minutes) which is a function of vehicle flow on road a and can be calculated in Eq.(4). Thus, $l_a / t_a \left(x_a\right)$ is the average travel speed of vehicles per unit of distance. $\varepsilon_1, \varepsilon_2$ are two coefficients in the vehicular emission function.

Therefore, the second objective of this decision-making problem is the total amount of vehicular air pollution emissions minimization from the perspective of sustainable transportation which can be expressed as follows:

$$\min_{\boldsymbol{\tau}} \quad Z_2 = \sum_{a_1 \in A_1} t_{a_1} \left(x_{a_1}, x_{a_2}\right) \exp\left(\varepsilon_2 \frac{l_{a_1}}{t_{a_1} \left(x_{a_1}, x_{a_2}\right)}\right) \left(x_{a_1} + x_{a_2}\right) \quad (73)$$

where Z_2 is the total air pollution emissions of all vehicles in the original network. t_{a_1} denotes the travel time cost on link a_1 in the extended network and the travel time cost of road a in the original network. Thus, $t_{a_1} \left(x_{a_1}, x_{a_2}\right) = t_a$ as shown in Eq.(4). Because the vehicle flow on road a equals to $x_{a_1} + x_{a_2}$ (i.e., $x_a = x_{a_1} + x_{a_2}$ in Eq.(2)), t_{a_1} is a function of link flow x_{a_1} and link flow x_{a_2}, which can be expressed as $t_{a_1} \left(x_{a_1}, x_{a_2}\right)$. Specifically, $t_{a_1} \left(x_{a_1}, x_{a_2}\right) = t_{a_1}^0 \left[1 + \alpha \left(\frac{x_{a_1} + x_{a_2}}{c_{a_1}}\right)^\beta\right]$ as calculated in Section 3.1.2. l_{a_1} is the length of link a_1 in the extended network, it equals to the length of road a in the original network, i.e., $l_{a_1} = l_a$. Due to the features of large capacity and low pollution, the air pollution emissions of the public transit vehicle and its change with the change of passenger flow are not taken into consideration.

3.3.2 Bi-objective bi-level optimization model

Based on the works accomplished above, the bi-level model can be formulated as follows:

(1) *Upper-level model:*

$$\min_{\boldsymbol{\tau}} \quad Z = \left\{ \begin{array}{c} \sum_{r^1 \in R^1} \sum_{s \in S} \sum_{k \in K^1} \sum_{p_k^{r^1 s} \in P_k^{r^1 s}} f_{p_k^{r^1 s}} \tilde{C}_{p_k^{r^1 s}} \left(\mathbf{f}, \boldsymbol{\lambda}, \tau^{rs}\right) + \sum_{r^1 \in R^1} \sum_{s \in S} \sum_{k \in K^0} \sum_{p_k^{r^0 s} \in P_k^{r^0 s}} f_{p_k^{r^0 s}} \tilde{C}_{p_k^{r^0 s}} \left(\mathbf{f}, \boldsymbol{\lambda}, \tau^{rs}\right) \\ \sum_{a_1 \in A_1} t_{a_1}\left(x_{a_1}, x_{a_2}\right) \exp\left(\varepsilon_2 \frac{l_{a_1}}{t_{a_1}\left(x_{a_1}, x_{a_2}\right)}\right)\left(x_{a_1} + x_{a_2}\right) \end{array} \right\} \tag{74}$$

s.t.

$$\underline{\tau}^{rs} < \tau^{rs} \leq \overline{\tau}^{rs}, \quad \forall r \in R, s \in S \tag{75}$$

where $\mathbf{f}$ and $\boldsymbol{\lambda}$ are implicitly defined by $MiCP(\mathbf{F})$ in **Definition 5**. Z denotes the bi-objective function of the upper-level model. $\boldsymbol{\tau}$ is the decision variable of traffic managers in the upper-level model as shown in Eqs.(53-54). $\overline{\tau}^{rs}$ is the upper bound of ridesharing compensation for OD pair rs, which represents the upper bound of the ridesharing payment for each rider or the upper-bound of ridesharing compensation to the ridesharing driver for picking up each rider between OD pair rs. $\underline{\tau}^{rs}$ is the lower bound of ridesharing compensation for OD pair rs.

(2) *Lower-level model:* $MiCP(\mathbf{F})$ in **Definition 5**.

Besides, the mixed complementarity problem $MiCP(\mathbf{F})$ in Section 3.2 which formulate heterogenous travelers' mode choice behavior is the lower-level model of this bi-level programming. The vector of path flow $\mathbf{f}$ and the vector of Lagrange multipliers $\boldsymbol{\lambda}$, $\boldsymbol{\mu}$ are decision variables of the lower-level model.

It is well recognized that the bi-level programming model is generally difficult to solve because the evaluation of the upper-level objective functions requires the solution of the lower-level subprogram (Szeto and Jiang, 2014; Li et al., 2017). Here, because the mixed complementarity formulation above can be replaced by the equivalent complementarity slackness conditions and additional nonnegativity constraints, the bi-level programming model can be straightforwardly transformed into a bi-objective single-level nonlinear programming problem which is a formulation of a mathematical program with complementarity constraints as follows:

$$\min_{\boldsymbol{\tau}, \mathbf{f}, \boldsymbol{\lambda}, \boldsymbol{\mu}} \quad Z = \left\{ \begin{array}{c} \sum_{r^1 \in R^1} \sum_{s \in S} \sum_{k \in K^1} \sum_{p_k^{r^1 s} \in P_k^{r^1 s}} f_{p_k^{r^1 s}} \tilde{C}_{p_k^{r^1 s}} \left(\mathbf{f}, \boldsymbol{\lambda}, \tau^{rs}\right) + \sum_{r^1 \in R^1} \sum_{s \in S} \sum_{k \in K^0} \sum_{p_k^{r^0 s} \in P_k^{r^0 s}} f_{p_k^{r^0 s}} \tilde{C}_{p_k^{r^0 s}} \left(\mathbf{f}, \boldsymbol{\lambda}, \tau^{rs}\right) \\ \sum_{a_1 \in A_1} t_{a_1}\left(x_{a_1}, x_{a_2}\right) \exp\left(\varepsilon_2 \frac{l_{a_1}}{t_{a_1}\left(x_{a_1}, x_{a_2}\right)}\right)\left(x_{a_1} + x_{a_2}\right) \end{array} \right\} \tag{76}$$

s.t.

$$\underline{\tau}^{rs} \leq \tau^{rs} \leq \overline{\tau}^{rs}, \quad \forall r \in R, s \in S \tag{77}$$

$$f_{p_1^{r^1 s}} \left(C_{p_1^{r^1 s}}\left(\mathbf{f}\right) + \frac{1}{\theta}(1 + \ln f_{p_1^{r^1 s}}) - \mu^{r^1 s} \right) = 0, \quad \forall p^{r^1 s} \in P^{r^1 s}, r^1 \in R^1, s \in S \tag{78}$$

$$C_{p_1^{r^1 s}}\left(\mathbf{f}\right) + \frac{1}{\theta}(1 + \ln f_{p_k^{r^1 s}}) - \mu^{r^1 s} \geq 0, \quad \forall p^{r^1 s} \in P^{r^1 s}, r^1 \in R^1, s \in S \tag{79}$$

$$f_{p_2^{r^1s}}\left(C_{p_2^{r^1s}}(\mathbf{f})+\frac{1}{\theta}(1+\ln f^*_{p_2^{r^1s}})+\lambda_+^{p^{rs}}-Cap\cdot\lambda_-^{p^{rs}}-\mu^{r^1s}\right)=0,\ \ \forall p^{rs}\in P^{rs}, r\in R, s\in S \tag{80}$$

$$C_{p_2^{r^1s}}(\mathbf{f})+\frac{1}{\theta}(1+\ln f_{p_2^{r^1s}})+\lambda_+^{p^{rs}}-Cap\cdot\lambda_-^{p^{rs}}-\mu^{r^1s}\geq 0,\ \ \forall p^{rs}\in P^{rs}, r\in R, s\in S \tag{81}$$

$$f_{p_3^{r^1s}}\left(C_{p_3^{r^1s}}(\mathbf{f})+\frac{1}{\theta}(1+\ln f_{p_3^{r^1s}})-\lambda_+^{p^{rs}}+\lambda_-^{p^{rs}}-\mu^{r^1s}\right)=0,\ \ \forall p^{rs}\in P^{rs}, r\in R, s\in S \tag{82}$$

$$C_{p_3^{r^1s}}(\mathbf{f})+\frac{1}{\theta}(1+\ln f_{p_3^{r^1s}})-\lambda_+^{p^{rs}}+\lambda_-^{p^{rs}}-\mu^{r^1s}\geq 0,\ \ \forall p^{rs}\in P^{rs}, r\in R, s\in S \tag{83}$$

$$f_{p_3^{r^0s}}\left(C_{p_3^{r^0s}}(\mathbf{f})+\frac{1}{\theta}(1+\ln f_{p_3^{r^0s}})-\lambda_+^{p^{rs}}+\lambda_-^{p^{rs}}-\mu^{r^0s}\right)=0,\ \ \forall p^{rs}\in P^{rs}, r\in R, s\in S \tag{84}$$

$$C_{p_3^{r^0s}}(\mathbf{f})+\frac{1}{\theta}(1+\ln f_{p_3^{r^0s}})-\lambda_+^{p^{rs}}+\lambda_-^{p^{rs}}-\mu^{r^0s}\geq 0,\ \ \forall p^{rs}\in P^{rs}, r\in R, s\in S \tag{85}$$

$$f_{p_4^{r^0s}}\left(C_{p_4^{r^0s}}(\mathbf{f})+\frac{1}{\theta}(1+\ln f_{p_4^{r^0s}})-\mu^{r^0s}\right)=0,\ \ \forall p_4^{r^0s}\in P_4^{r^0s}, r^0\in R^0, s\in S \tag{86}$$

$$C_{p_4^{r^0s}}(\mathbf{f})+\frac{1}{\theta}(1+\ln f_{p_4^{r^0s}})-\mu^{r^0s}\geq 0,\ \ \forall p_4^{r^0s}\in P_4^{r^0s}, r^0\in R^0, s\in S \tag{87}$$

$$\lambda_+^{p^{rs}}\left(f_{p_3^{r^1s}}+f_{p_3^{r^0s}}-f_{p_2^{r^1s}}\right)=0,\ \ \forall p^{rs}\in P^{rs}, r\in R, s\in S \tag{88}$$

$$f_{p_3^{r^1s}}+f_{p_3^{r^0s}}-f_{p_2^{r^1s}}\geq 0,\ \ \forall p_3^{rs}\in P_3^{rs}, p_2^{r^1s}\in P_2^{r^1s}, r\in R, s\in S \tag{89}$$

$$\lambda_-^{p^{rs}}\left(Cap\cdot f_{p_2^{r^1s}}-f_{p_3^{r^1s}}-f_{p_3^{r^0s}}\right)=0,\ \ \forall p^{rs}\in P^{rs}, r\in R, s\in S \tag{90}$$

$$Cap\cdot f_{p_2^{r^1s}}-f_{p_3^{r^1s}}-f_{p_3^{r^0s}}\leq 0,\ \ \forall p_3^{rs}\in P_3^{rs}, p_2^{r^1s}\in P_2^{r^1s}, r\in R, s\in S \tag{91}$$

$$\left(f_{p_2^{r^1s}}\cdot v_{p^{rs}}-\left(f_{P_3^{r^1s}}+f_{P_3^{r^0s}}\right)+\lambda_{v-}^{p^{rs}}\right)\left(v_{p^{rs}}-1\right)=0,\ \ \forall p^{rs}\in P^{rs}, r\in R, s\in S \tag{92}$$

$$f_{p_2^{r^1s}}\cdot v_{p^{rs}}-\left(f_{p_3^{r^1s}}+f_{p_3^{r^0s}}\right)-\lambda_{v-}^{p^{rs}}\geq 0,\ \ \forall p^{rs}\in P^{rs}, r\in R, s\in S \tag{93}$$

$$\lambda_{v-}^{p^{rs}}\left(Cap-v_{p^{rs}}\right)=0,\ \ \forall p^{rs}\in P^{rs}, r\in R, s\in S \tag{94}$$

$$1\leq v_{p^{rs}}\leq Cap,\ \ \forall p^{rs}\in P^{rs}, r\in R, s\in S \tag{95}$$

$$\sum_{k\in K^1}\sum_{p_{a_k}^{r^1s}\in P_{a_k}^{r^1s}} f_{p_{a_k}^{r^1s}}-q^{r^1s}=0,\ \ \forall r^1\in R^1, s\in S \tag{96}$$

$$\sum_{k\in K^0}\sum_{p_{a_k}^{r^0s}\in P_{a_k}^{r^0s}} f_{p_{a_k}^{r^0s}}-q^{r^0s}=0,\ \ \forall r^0\in R^0, s\in S \tag{97}$$

$$\mathbf{f},\boldsymbol{\lambda}\geq 0 \tag{98}$$

where $\boldsymbol{\tau}$, $\mathbf{f}$, $\boldsymbol{\lambda}$, $\boldsymbol{\mu}$ are the decision variables of the above single-level nonlinear programming model. Eqs.(78-98) are the equivalent complementarity slackness conditions and additional nonnegativity constraints corresponding to the mixed complementarity problem $MiCP(\mathbf{F})$ in Eqs.(60-70).

4 Solution procedure

Solving the compensation optimization model in Section 3.3.2, there are two difficulties have to deal with: the bi-objective function and complementarity constraints.

First, as a bi-objective optimization model, previous related studies have proven that the relationship between the ridesharing compensation and urban traffic conditions is not simply

monotonic but rather complex (Wang et al., 2018; Xu, Pang, Ordónez and Dessouky, 2015; Yan et al., 2019). Vehicular air pollution emissions do not keep increasing with the increase of travel speed (Yin and Lawphongpanich, 2006). Thus, different objectives conflict with each other, and the optimal parameters of one objective usually do not lead to the optimality of another objective. Besides, total generalized travel cost Z_1 and the total amount of vehicular air pollution emissions Z_2 in Section 3.3.1 are two objective functions from the perspective of the efficiency of urban traffic system and sustainable transportation respectively. They are differently measured and scaled objectives, therefore, it is difficult to transform into comparable units. Thus, a set of Pareto-optimal solutions must be found instead of one single solution. As a widely used method for multi-objective optimization, Non-Dominated Sorting Genetic Algorithm II (NSGA-II) can be applied to obtain an efficient Pareto frontier of ridesharing compensation for minimizing the total travel cost and vehicular air pollution emissions (Deb et al., 2002). Second, as a mathematical program with complementarity constraints, due to the non-convex feasible region caused by the complementarity constraints, the nonlinear multivariate travel cost, and the non-concave objective function, it is challenging to solve directly (Ban et al., 2006; Noruzoliaee et al., 2018). However, under the given ridesharing compensation τ, solutions $\mathbf{f}, \boldsymbol{\lambda}, \boldsymbol{\mu}$ that satisfy the complementarity constraints can be obtained by solving the mixed complementarity problem $MiCP(\mathbf{F})$. Meanwhile, the mixed complementarity problem $MiCP(\mathbf{F})$ can be solved by the PATH solver which is an efficient solver built-in GAMS for non-linear complementarity problems (Brook et al., 1988).

Therefore, in this section, an improved NSGA-II with the combination of solving the mixed complementarity problem is developed to solve the bi-objective nonlinear programming model (Deb et al., 2002). The main steps of solution process is illustrated as follows:

Step 1 *Initialization.*

Step 1.1 Determining the number of chromosomes in the population n, the maximum number of generations M, the probabilities of crossover P_c and mutation P_m, etc.

Step 1.2 Randomly generate an initial vector P_0 which contain n feasible ridesharing compensations $\boldsymbol{\tau}$. An offspring vector S_0 is generated from the vector of parents P_0 using the standard genetic algorithms. Set the number of generations equal to zero, $t = 0$.

Step 2 *Non-dominated sorting.*

Step 2.1 Both P_t and S_t are merged into a vector R_t of size $2n$, i.e., $R_t = P_t \cup S_t$. Each element in vector R_t represents a feasible ridesharing compensation $\boldsymbol{\tau}$. For each feasible ridesharing compensation $\boldsymbol{\tau}$ in vector R_t, obtain the path flow pattern $\mathbf{f}$ that satisfy complementarity slackness conditions and additional nonnegativity constraints in Eqs.(77-96) through solving the mixed complementarity problem $MiCP(\mathbf{F})$ by the PATH solver in GAMS. Then, the vector R_t, the corresponding vector of path flow $\mathbf{f_t}$, and the corresponding vector of Lagrange multipliers $\boldsymbol{\lambda_t}$ compose population W_t (i.e., each chromosome in population W_t represents a feasible solution for the bi-objective single-level nonlinear programming problem in Section 3.3.2).

Step 2.2 Implement the fast-non-dominated sorting for population W_t. Evaluating the two objectives (i.e., Z_1 and Z_2 in Section 3.3.1) for each chromosome in population W_t. According to the dominance relationship among solutions, classify all individual solutions into different dominance levels $F_i\,(i = 1, 2, \cdots)$ (i.e., Pareto ranks, Pareto fronts) and calculate the crowding distance D_{ij} for solution j in dominance level F_i.

Step 3 *Tournament selection.*

Implement the tournament selection for population W_t based on dominance rank F_i and crowding distance D_{ij}. The new population P_{t+1} is filled by different nondominated solutions in population W_t. Note that because the number of chromosomes in population W_t is $2n$, only half of it will be put into the new population P_{t+1}. Selecting nondominated solutions in population W_t according to the ascending order of dominance levels, i.e., $F_1, F_2, \cdots$. For nondominated solutions in the same dominance level F_i, selecting nondominated solutions in descending order of crowding distances D_{ij}.

Step 4 *Offspring generation.*

A new offspring vector S_{t+1} is generated after the implementation of selection, the simulated binary crossover with a certain probability P_c, and the polynomial mutation with a certain probability P_m.

Step 5 *Stopping criteria.*

Stop, if the number of generations t is equal to the maximum generation M or Pareto front unchanged. Otherwise, back to Step 2.

For a clear description, the brief pseudo-code for the improved NSGA-II is presented in Algorithm 1.

5 Numerical experiments

In this section, two networks will be used to conduct numerical experiments, i.e., a single corridor network (single OD pair with single path), Nguyen and Dupuis's network (multiple OD pairs with multiple paths). Specifically, a single corridor network will be adopted to analyze the impact of the value of ridesharing compensation on the performance of urban traffic systems with the introduction of ridesharing programs. Moreover, the impact of subsidy policy on urban traffic conditions and pollution emissions in the early days of ridesharing will also be analyzed. Then, we use Nguyen and Dupuis's network to demonstrate the properties of the optimization problem, the performance of our established model and the proposed algorithm. A set of comparative experiments will be conducted to demonstrate the necessity of considering the stochasticity of generalized travel cost (i.e., limited perceived ability of travelers) in the modeling of the ridesharing compensation optimization problem. Besides, a set of sensitivity experiments is carried out to investigate the impact of the value of ridesharing capacity on the Pareto-optimal solutions and Pareto-efficient frontier.

Algorithm 1 Brief pseudo-code for the improved NGSA-II.

Generate an initial vector P_0 which contain n feasible ridesharing compensations
Generate an offspring vector S_0 using the standard genetic algorithms
$t = 0$
while stopping criteria is not reached **do**
  $R_t = P_t \cup S_t$
  $[\mathbf{f_t}, \boldsymbol{\lambda_t}]$ = Solving $MiCP\left(\mathbf{F}\left(\mathbf{R_t}\right)\right)$ by PATH solver in GAMS
  $W_t = \{R_t, \mathbf{f_t}, \boldsymbol{\lambda_t}\}$
  $[\mathbf{F}, \mathbf{D}]$ = fast-non-dominated-sort(W_t)
  $P_{t+1} = \emptyset$ and $i = 1$
  while $|P_{t+1}| + |F_i| \leqslant n$ **do**
    F_i = crowding-distance-sort(F_i) in descending order of D_{ij}
    $P_{t+1} = P_{t+1} \cup F_i$
    $i = i + 1$
  end while
  $Sort\left(F_i, \prec_n\right)$ where $\prec_n$ is the crowded-comparison operator (Deb et al., 2002)
  $P_{t+1} = P_{t+1} \cup F_i\left[1 : (n - |P_{t+1}|)\right]$
  S_{t+1} = generate-new-offspring(P_{t+1}) after selection, crossover, and mutation
  $t = t + 1$
end while

5.1 Single corridor network

Consider a single corridor network that consists of a road a and a public transit line b that runs in parallel. In the original network, there is a single original node r and a single destination node s. After constructing the extended network as described in Section 2.3, we set the travel demand between OD pair r^1s and rs equals to the number of car-owners and non-car owners which is exogenously given by $q^{r^1s} = 150$, $q^{r^0s} = 150$. Besides, all other parameters of the numerical experiments based on the single corridor network are listed in Table 3.

Table 3: List of parameters

Parameters	Description	Value
α, β	Parameters of the BPR function	0.15, 4
η_1, η_0	VOT of car owners and non-car owners	40\$/h, 20\$/h
θ	Parameter of the perceptual error	0.068
t_a^0	Free-flow travel time of road a	0.6h
c_a	Capacity of road a	150
l_a	Length of road a	36km
h	Vehicle fuel cost of per hour	20
t_b^0	Fixed running time of the public transit vehicle on line b	1h
H_b	Departure headway of public transit line b	5min
c_b	Capacity of public transit vehicles on line b	75
τ^{PT}	Fare cost for riders on public transit line	2
Cap	Capacity of each ridesharing vehicle	3
Δ	Inconvenience cost caused by sharing a vehicle with others	3
$\varepsilon_1, \varepsilon_2$	Parameters in the vehicular emission function	0.2038, 0.7962

5.1.1 Ridesharing compensation analysis

Because there is only one OD pair in the single corridor network, a set of sensitivity experiments is carried out to analyze the change of the total generalized travel cost and vehicular air pollution emissions under the generalized SUE as the ridesharing compensation vary. Specifically, by varying the ridesharing compensation τ^{rs} from 0 to 16 and solving the corresponding mixed complementarity problem $MiCP(\mathbf{F})$ in **Definition 5**, results of the total generalized travel cost and vehicular air pollution emissions can be calculated according to Eqs.(71-73) and illustrated as follows:

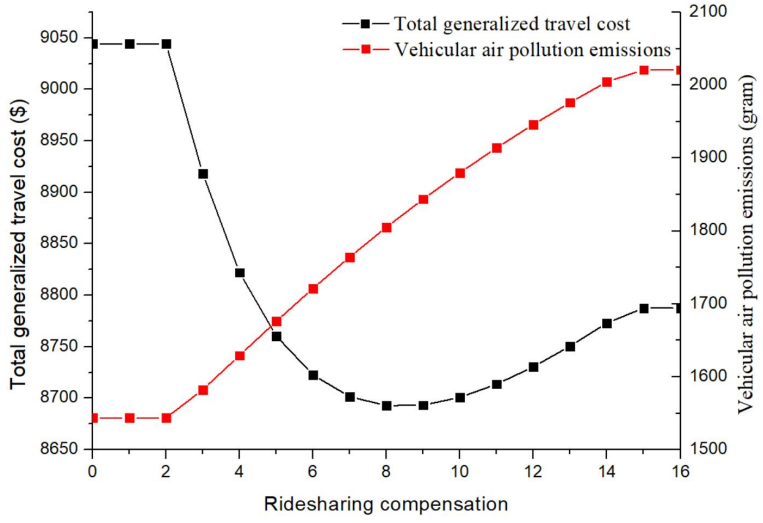

Figure 4: Change of the total generalized travel cost and vehicular air pollution emissions with the increase of ridesharing compensation

From an overall perspective, the relationship between the total generalized travel cost and the ridesharing compensation is not simply monotonic but rather complex even in a single corridor network. Specifically, as illustrated in Figure 4, the total generalized travel cost decreases firstly and then increases with the increase of ridesharing compensation, while vehicular air pollution emissions keep monotonically increasing with the increase of ridesharing compensation. It indicates the total generalized travel cost minimization and vehicular air pollution emissions minimization are two objectives that generally conflict with each other. Both the complex relationship between objectives and the value of ridesharing compensation, and the conflict between two different objectives make it is necessary to provide a methodology to supply a set of Pareto-optimal solutions for policy-makers rather than a single decision-making strategy, especially in a more complex urban traffic network. Besides, because the value of ridesharing compensation directly determines the cost that travelers participate in the ridesharing program, with the ridesharing compensation increasing from 2 to 14, the number of ridesharing drivers keeps increasing and the number of ridesharing riders keeps decreasing as shown in Figure 5.

Moreover, it is worth noting that when the ridesharing compensation varies within the range 0-2 or 15-16, both the total generalized travel cost and vehicular air pollution emissions keep unchanged. The specifical reason can be explained according to the **Proposition 2** in Section 3.2.1. When the basic ridesharing compensation $\tau^{rs} = 0$, it has $\lambda_+ = 0, \lambda_- = 2.13$. Therefore, based on the **Proposition 2**, we can derive that the basic ridesharing compensation τ^{rs} varies within the range of $[0, 2.13]$ will not change the actual ridesharing payment and compensation since the ridesharing market can adjust the value of ridesharing compensation/payment reduction (i.e., λ_- as shown in Figure 5) to balance the number of ridesharing supply and ridesharing demand. Finally, both the actual ridesharing payment and the actual ridesharing compensation are the same and equal to 2.13. Meanwhile, the number of drivers and riders in the ridesharing system keeps unchanged and reaches the upper bound constraint in Eq.(17) as shown in Figure 5, i.e., the number of ridesharing riders reaches the capacity of all ridesharing drivers can pick up. Thus, the total generalized travel cost and vehicular air pollution emissions keep unchanged.

Similarly, when the basic ridesharing compensation $\tau^{rs} = 16$, it has $\lambda_+ = 1.40, \lambda_- = 0$. Therefore, based on the **Proposition 2**, we can know that the basic ridesharing compensation τ^{rs} varies within the range of $[14.60, +\infty)$ will not change the actual ridesharing payment and compensation. The actual ridesharing payment for each rider and the actual ridesharing compensation for each driver are equal to 14.6 and 43.8 respectively. Because if the number of ridesharing participants already reaches the upper bound constraint in Eq.(17) and we still increase the basic ridesharing compensation/payment, the ridesharing market will adjust the value of ridesharing compensation/payment reduction (i.e., λ_- as shown in Figure 5) to guarantee the actual ridesharing compensation/payment unchanged and balance the number of ridesharing supply and ridesharing demand. Meanwhile, the number of drivers and riders in the ridesharing system keeps unchanged and reaches the lower bound constraint in Eq.(16) as shown in Figure 5, i.e., the number of ridesharing riders is equal to the number of ridesharing drivers. Thus, the total generalized travel cost and vehicular air pollution emissions keep unchanged.

To summarize the above results, we can find that when the number of ridesharing participants does not reach the lower bound and the upper bound constraint, the actual ridesharing compensation/compensation is equal to the basic ridesharing compensation/compensation which is

determined according to a pre-specified pricing scheme. However, if the number of ridesharing participants reaches the lower/upper bound constraint in Eqs.(16-17) and the basic ridesharing compensation within a certain range as described in **Proposition 2**, the actual ridesharing compensation/compensation does not equal to the basic ridesharing compensation/compensation anymore. Finally, the actual ridesharing compensation/compensation keeps unchanged and determined by the ridesharing market itself.

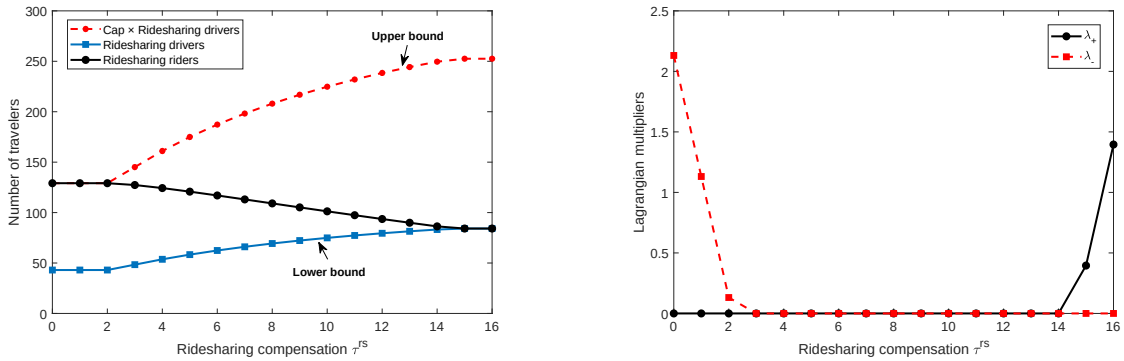

Figure 5: Change of the number of ridesharing participants and Lagrangian multipliers with the increase of ridesharing compensation

5.1.2 Subsidy policy analysis

It is well-known to all that the money-burning subsidy strategy is a popular tactic employed by TNCs (e.g., Uber, Lyft, and DiDi) in the early days of ridesharing. To encourage travelers to participate in the emerging ridesharing program, TNCs gives attractive subsidies to all ridesharing participants, both ridesharing drivers and ridesharing riders. Ridesharing subsidies can change travelers' mode choice behavior by directly decreasing the travel cost of ridesharing participants which further affects urban traffic conditions.

Thus, we conduct sensitivity experiments to analyze the impact of different amount of ridesharing subsidies on travelers' mode choice and urban traffic systems under the generalized SUE. Here, the ridesharing compensation/payment between OD pair rs is a constant which is exogenously given by $\tau^{rs} = 15$. Let σ^d and σ^p represent the subsidy that TNCs give to the ridesharing driver and the ridesharing rider for each travel respectively. For simplicity, let $\sigma^d = \sigma^p$. Thus, the travel cost of ridesharing drivers and riders (i.e., $C_{p_2^{r^1 s}}, C_{p_3^{r^1 s}}, C_{p_3^{r^0 s}}$) in Section 3.1.2 can be updated as the following equations.

$$\begin{cases} C_{p_2^{r^1 s}}^{Update} = C_{p_2^{r^1 s}} - \sigma^d \\ C_{p_3^{rs}}^{Update} = C_{p_3^{rs}} - \sigma^p, \quad \forall r \in \{r^1, r^0\} \end{cases}$$

After taking it into the mixed complementarity problem formulation of SUE model $MiCP(\mathbf{F})$ in **Definition 5**, travel mode choices at SUE corresponding to the updated travel cost $C_{p_2^{r^1 s}}^{Update}$, $C_{p_3^{r^1 s}}^{Update}$, $C_{p_3^{r^0 s}}^{Update}$ can be calculated out. Moreover, sensitivity experiments are conducted by varying the

value of ridesharing subsidies σ^d, σ^p from 0 to 15. The change of travel mode choices at SUE, the total generalized travel cost, vehicular air pollution emissions, and the total amount of subsidy paid by TNCs as the value of ridesharing subsidy varies (i.e., σ^d, σ^p) is illustrated in Figure 6.

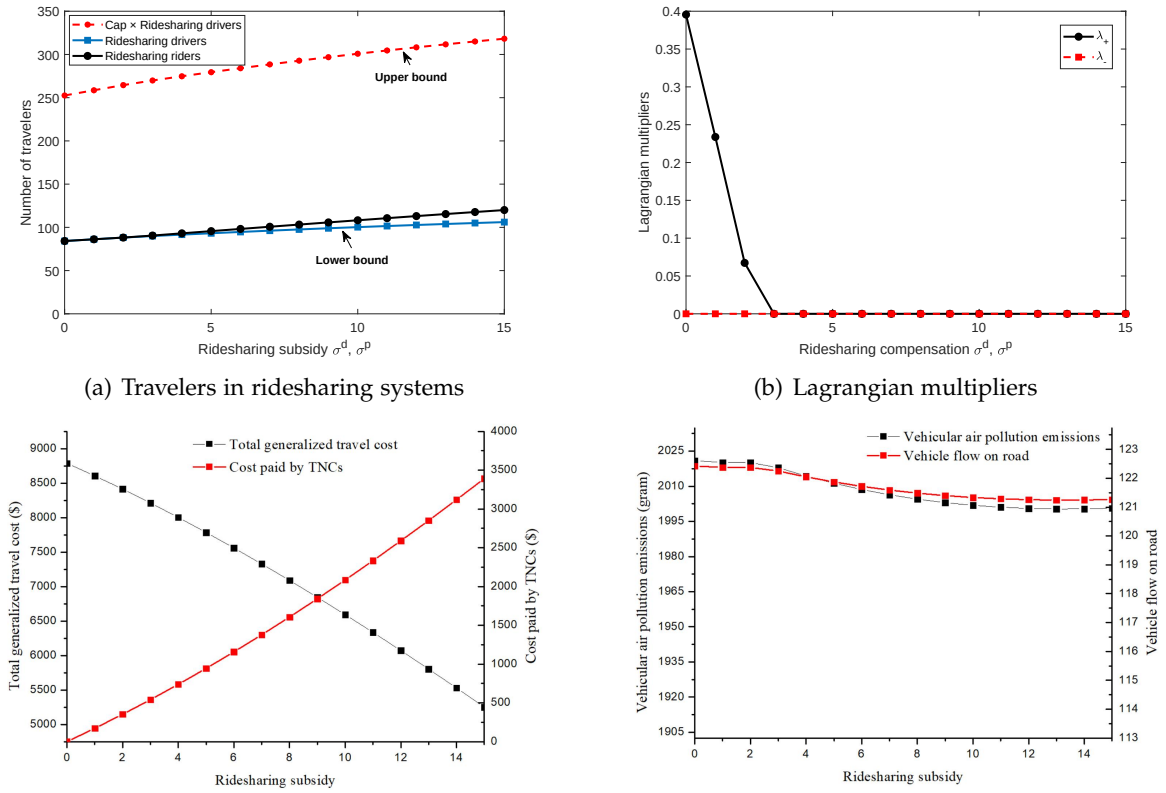

(a) Travelers in ridesharing systems

(b) Lagrangian multipliers

(c) Vehicular air pollution emissions

(d) Vehicle flow

Figure 6: Change of various indices with the increase of ridesharing subsidy

As shown in Figure 6(a), the ever-increasing subsidy attracts a growing number of drivers and riders participanting in the ridesharing programs by directly decreasing their generalized travel cost. Meanwhile, a more rapid increase is observed in the number of ridesharing riders. It indicates compared with ridesharing drivers, ridesharing subsidies are more attractive to ridesharing riders.

When the ridesharing subsidy varies in the range of 0-2, the number of drivers and riders in the ridesharing system reaches the lower bound constraint with equality in Eq.(16), i.e., the number of ridesharing drivers is equal to the number of ridesharing riders as shown in Figure 6(a). Besides, there is always a ridesharing payment reduction for each ridesharing rider (i.e., $\lambda_+ > 0$). The actual ridesharing payment for ridesharing riders is less than the basic ridesharing payment. Meanwhile, ridesharing drivers also suffer a ridesharing compensation reduction. Without the payment reduction λ_+ in the ridesharing compensation/payment, there will be more travelers who intend to be ridesharing drivers but cannot be matched with ridesharing riders due to the shortage of ridesharing riders. Therefore, the positive ridesharing compensation/payment reduction λ_+ the balance between ridesharing supply and ridesharing demand. However, when the value of ridesharing subsidy is greater than 3, no ridesharing compensation/payment reduction

is needed anymore since the number of ridesharing riders exceeds the number of ridesharing drivers.

As illustrated in Figures 6(c) and 6(d), the ridesharing subsidy can indeed reduce the vehicle flow on the road, the total generalized travel cost, and vehicular air pollution emissions in urban traffic systems with the introduction of ridesharing programs. But there is a much difference among their reduction. Specifically, with the increase of ridesharing subsidy, the total generalized travel cost of the urban traffic systems has significantly decreased, while the vehicle flow on the road and vehicular air pollution emissions only have a slight decrease. What's more, the increment of the cost paid by TNCs is much higher than the decrement of the total generalized travel cost as shown in Figure 4(c). It indicates there is a significant improvement in urban traffic conditions and a slight decrease in vehicular air pollution emissions at the cost of huge subsidy provided by TNCs, but high-intensity subsidies are not a continuous and sustainable way to promote the development of ridesharing services.

5.2 Nguyen and Dupuis's network

The single corridor network is relatively simple which only consists of one OD pair, one single road, and one public transit line. The route choice behavior, the interaction among travelers of different OD pairs, and different ridesharing compensations among different OD pairs have not been taken into account in the formulation. Here, Nguyen and Dupuis's network (Nguyen and Dupuis, 1984) as shown in Figure 7 is used to demonstrate the properties of the optimization problem and the performance of our proposed model.

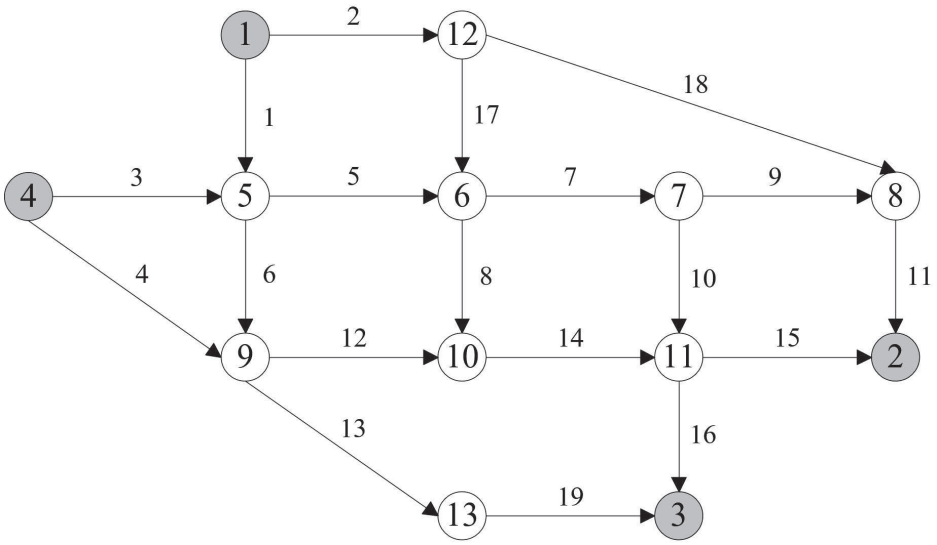

Figure 7: Nguyen and Dupuis's network

This example network consists of 13 nodes, 19 links, and 4 OD pairs (1–2, 1–3, 4–2, and 4–3). The numbers of paths between those OD pairs are 8, 6, 5, and 6 respectively. There are two origin nodes (Zones 1, 4) and two destination nodes (Zones 2, 3) among all nodes, i.e., $R = \{1,4\}$, $S = \{2,3\}$. We assume there are a road and a public transit line between any two adjacent nodes as described in Section 2.1. Moreover, the parameters of each link (i.e., each road

and each public transit line) and the existing OD matrix of travel demand are listed in Table 4 and Table 5 respectively, which are taken from (Xu et al., 2011; Li et al., 2017). The capacity of public transit vehicles on each line equals to 150, i.e., $c_b = 150$, $\forall b \in B$. Set the lower bound of ridesharing compensation $\underline{\tau}^{rs}$ for OD pair rs equal to zero and the upper bound of ridesharing compensation $\overline{\tau}^{rs}$ for OD pair rs equal to 15, i.e., $\underline{\tau}^{rs} = 0, \overline{\tau}^{rs} = 15$.

Table 4: Link properties for Nguyen and Dupuis's network

Link	Road capacity (veh/h)	Free-flow travel time (min)	Road length (km)	Fixed running time of the public transit line (min)
1	300	7	8.75	11.67
2	200	9	11.25	15
3	200	9	11.25	15
4	200	12	15	20
5	350	3	3.75	5
6	400	9	11.25	15
7	500	5	6.25	8.33
8	250	13	16.25	21.67
9	250	5	6.25	8.33
10	300	9	11.25	15
11	500	9	11.25	15
12	550	10	12.5	16.67
13	200	9	11.25	15
14	400	6	7.5	10
15	300	9	11.25	15
16	300	8	10	13.33
17	200	7	8.75	11.67
18	300	14	17.5	23.33
19	200	11	13.75	18.33

Table 5: Travel demand distribution of heterogenous travelers

OD pair	Car owners	Non-car owners
1-2	330	330
1-3	247	247
4-2	206	206
4-3	247	247

After constructing the extended network, we have 70 nodes, 152 links, and 8 OD pairs. The numbers of paths between those OD pairs are 40, 30, 25, and 30 respectively. The basic prosperities of the extended network (e.g., link capacity c_{a_k}, free-flow travel time $t^0_{a_k}$, the travel demand distribution $q^{r^1 s}, q^{r^0 s}$, etc) can be derived from the original network according to the description in Section 2.3.

For the NGSA-II algorithm, the number of chromosomes in the population $n = 100$, the maximum number of generations $M = 200$, or the algorithm terminates when the Pareto-efficient frontier is unchanged after 5 iterations, the probabilities of crossover $P_c = 0.9$ and mutation $P_m = 0.1$. Keep other parameters identical to the numerical experiments in Section 5.1.

Based on the above setup, we perform the optimization methodology for ridesharing compensation in Nguyen and Dupuis's network. The convergence and stability of the proposed algorithm can be illustrated in Figure 8 which gives out Pareto-optimal solutions for Nguyen and Dupuis's network case study. The lateral axis represents the total generalized travel cost Z_1, and the vertical axis represents the total amount of vehicular air pollution emissions Z_2.

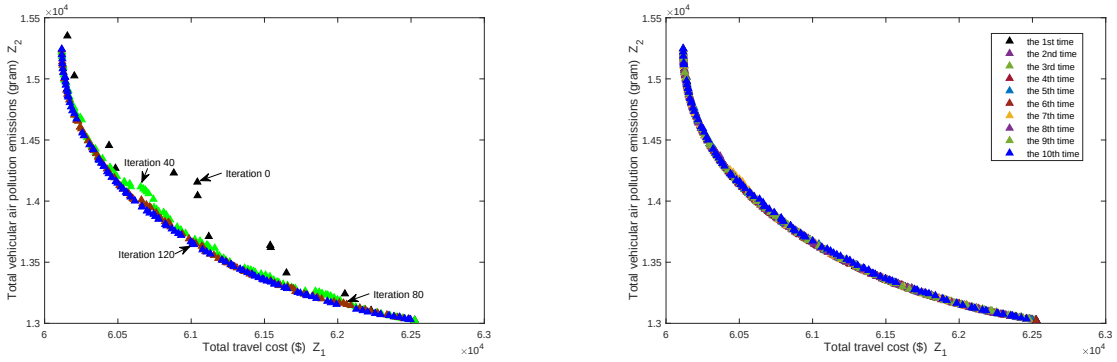

(a) Value of objective functions of non-dominated solutions in the first rank for every forty generations

(b) Pareto-efficient frontier for each run

Figure 8: Pareto-optimal solutions for the Nguyen and Dupuis's network case study

For the convergence of the proposed algorithm, Figure 8(a) shows the value of objective functions of non-dominated solutions in the first rank for every forty generations. It is found that, compared with the value of objective functions of the initial population, both the total generalized travel cost and the total amount of vehicular air pollution emissions have significantly decreased with the increase of iteration times. Finally, the value of objective functions of non-dominated solutions in the first rank remains unchanged after 120 iterations. It indicates one set of Pareto optimal solutions are generated, i.e., the blue points in Figure 8(a). These solutions provide a Pareto-efficient frontier (e.g., Pareto front) for policy-makers and allow them to choose desired solutions.

Moreover, to demonstrate the stability of the proposed algorithm, the numerical experiment has been run 10 times with different initial populations independently. The value of objective functions of Pareto optimal solution sets for each run has been illustrated in Figure 8(b). It is shown that Pareto optimal solution sets for each run converge to the same objective space, namely different initial population derives the same Pareto-efficient frontier.

Table 6: Pareto optimal solutions corresponding to Figure 8(a)

Solutions / OD pair	1	2	3	4^*	5^*	6^*
1-2	1.78	3.49	5.80	8.90	1.23	1.24
1-3	1.42	3.46	5.94	8.28	0.41	1.58
4-2	1.93	3.14	6.37	7.38	0.61	1.48
4-3	2.32	3.21	5.31	7.80	0.50	1.47
Total generalized travel cost ($\times 10^4$)	6.23	6.13	6.03	6.01	6.25	6.25
Vehicular air pollution emissions ($\times 10^4$)	1.31	1.35	1.44	1.52	1.30	1.30

Table 6 gives some examples of Pareto optimal solutions in Figure 8(a). Compared with chromosomes in the initial population, all solutions simultaneously improve urban traffic congestions and pollution emissions. It is worth noting that 4^* is also the solution of the single-objective optimization model with objective Z_1 (total generalized travel cost minimization). It makes the urban traffic system has the lowest total generalized travel cost but higher vehicular air pollution emissions. 5^* and 6^* are solutions of the single-objective optimization model with objective Z_2 (vehicular air pollution emissions minimization). Contrary to solution 4^*, they make the urban traffic system has the lowest vehicular air pollution emissions but a higher total generalized travel cost. It is illustrated that two objectives are generally in conflict with each other. Thus, for the decision-making problem of ridesharing compensation, Pareto optimal solutions calculated in this study can provide more flexibility for policy-makers than a single optimization solution calculated by the single-objective optimization model. Moreover, we find that the single-objective optimization model with objective Z_2 has alternative optimal solutions. To analyze the specific reason, the path-related information for OD pair 4-2 corresponding to solutions 5^* and 6^* is listed in Table 7 and Table 8 respectively.

Table 7: Path-related information for OD pair 4-2 corresponding to solutions 5^*

Path properties	Path 1	Path 2	Path 3	Path 4	Path 5
Node sequence	3-5-7-9-11	3-5-8-14-15	3-5-7-10-15	3-6-12-14-15	4-12-14-15
$\lambda_+^{p^{rs}}$	0	0	0	0	0
$\lambda_-^{p^{rs}}$	0.87	2.10	1.44	2.47	1.52
Actual ridesharing payment	1.48	2.72	2.05	3.08	2.14
Solo drivers	20.50	10.76	15.21	8.96	14.57
Ridesharing drivers	15.05	10.16	12.54	9.10	12.21
Ridesharing riders(Car owners)	20.99	12.56	16.55	10.85	15.99
Ridesharing riders(Non-car owners)	24.18	17.93	21.06	16.46	20.64
Public transit riders	26.22	18.66	22.54	16.66	21.65

Table 8: Path-related information for OD pair 4-2 corresponding to solutions 6^*

Path properties	Path 1	Path 2	Path 3	Path 4	Path 5
Node sequence	3-5-7-9-11	3-5-8-14-15	3-5-7-10-15	3-6-12-14-15	4-12-14-15
$\lambda_+^{p^{rs}}$	0	0	0	0	0
$\lambda_-^{p^{rs}}$	0	1.23	0.57	1.59	0.65
Actual ridesharing payment	1.48	2.72	2.05	3.08	2.14
Solo drivers	20.50	10.76	15.21	8.96	14.57
Ridesharing drivers	15.05	10.16	12.54	9.10	12.21
Ridesharing riders(Car owners)	20.99	12.56	16.55	10.85	15.99
Ridesharing riders(Non-car owners)	24.18	17.93	21.06	16.46	20.64
Public transit riders	26.22	18.66	22.54	16.66	21.65

We find that the number of ridesharing participants on each path between all OD pairs corresponding to solution 5^* and 6^* reaches the upper bound constraint in Eq.(17). Namely, for each path between all OD pairs, the number of ridesharing riders reaches the capacity that all ridesharing drivers can pick up. Meanwhile, for the solution 5^*, the basic ridesharing compensation $\tau^{4-2} = 0.61$, thus we can derive

$$\tau^{4-2} + \min_{p^{4-2} \in P^{4-2}} \lambda_-^{p^{4-2}*} = 0.61 + \min\{0.87, 2.10, 1.44, 2.47, 1.52\} = 1.48.$$

Similarly, $\tau^{1-2} + \min_{p^{1-2} \in P^{1-2}} \lambda_-^{p^{1-2}*} = 1.24$, $\tau^{1-3} + \min_{p^{1-3} \in P^{1-3}} \lambda_-^{p^{1-3}*} = 1.58$, $\tau^{4-3} + \min_{p^{4-3} \in P^{4-3}} \lambda_-^{p^{4-3}*} = 1.47$. Therefore, based on the **Proposition 2**, we can know that the basic ridesharing compensation τ^{1-2} varies within the range of $[0, 1.24]$, τ^{4-2} varies within the range of $[0, 1.58]$, τ^{1-3} varies within the range of $[0, 1.48]$, and τ^{4-3} varies within the range of $[0, 1.47]$ will not change the ridesharing payment, the generalized SUE, the total generalized travel cost, and the vehicular air pollution emissions. Therefore, the single-objective optimization model with objective Z_2 has alternative optimal solutions. Naturally, although solution 5^* and solution 6^* have different values of the basic ridesharing compensation τ^{rs}, they have the same actual ridesharing payment and compensation, and the same path flow pattern, etc.

As illustrated in Tables 7-9, compared with the link-based modeling method, the path-based modeling method in this study not only can obtain the link flow pattern under the generalized SUE but also can directly list the route information of all travelers. Besides, for previous studies (Xu, Pang, Ordónez and Dessouky, 2015; Di et al., 2018), the constraints on the number of ridesharing drivers and the number of ridesharing riders are given in the form of the link flow. It only limits the number of ridesharing participants on each link should satisfy the constraints on ridesharing supply and ridesharing demand. Travelers are allowed to change their mode choices for a single trip. Ridesharing riders are allowed to take several ridesharing vehicles in turns (i.e., several transfers) for a single trip. That is not consistent with reality. However, the above shortcomings of the link-based formulation are overcome in this study by adopting the path-based constraints. It can be checked that not only the path flow in Table 7 and Table 8 satisfies the lower bound constraint and the upper bound constraint in Eqs.(16-17), but also the link flow in Table 9 satisfies the constraints on ridesharing supply and ridesharing demand.

As described in Section 1, the modeling of travelers' choice behavior in all previous related literature is based on Wardrop's UE principle. Specifically, in the urban traffic system with the introduction of ridesharing programs, they assume all travelers know urban traffic conditions very well and choose the travel mode/route whose generalized travel cost is the smallest. Here, a comparative experiment in which travelers make their mode and route choice decisions based on the UE principle has been conducted to analyze the decision-making problem of ridesharing compensation under the UE principle. Since UE is just a special case of SUE, after setting the parameter of perceptual error $\theta = +\infty$ in Section 3.3 (i.e., delete the item $\frac{1}{\theta}(1 + \ln f_{p_k^{rs}})$ in Eqs.(76-98)), we can obtain a new compensation optimization model which integrates travelers' choice behavior based on UE principle. keep all other parameters unchanged. Then, after implementing the proposed algorithm in Section 4, a set of Pareto-optimal solutions for the comparative experiment can be calculated after 150 iterations as shown in Figure 9(a). Due to the limited perceived ability of travelers, there is always a perceptual error when they make travel choice decisions in reality. Therefore, to further appraise the actual performance of decision-making strategies in the comparative experiment, the value of objective functions corresponding to Pareto-optimal solutions in Figure 9(a) is recalculated by solving $MiCP(\mathbf{F})$ in **Definition 5** and illustrated by the red points in Figure 9(b). After taking the Pareto-efficient frontier of this study as a benchmark (i.e., blue points in Figure 9(b)), it is intuitively shown the total generalized travel cost and total vehicular air pollution emissions of urban traffic systems in reality if policy-makers adopt the decision-making strategies in the comparative experiment.

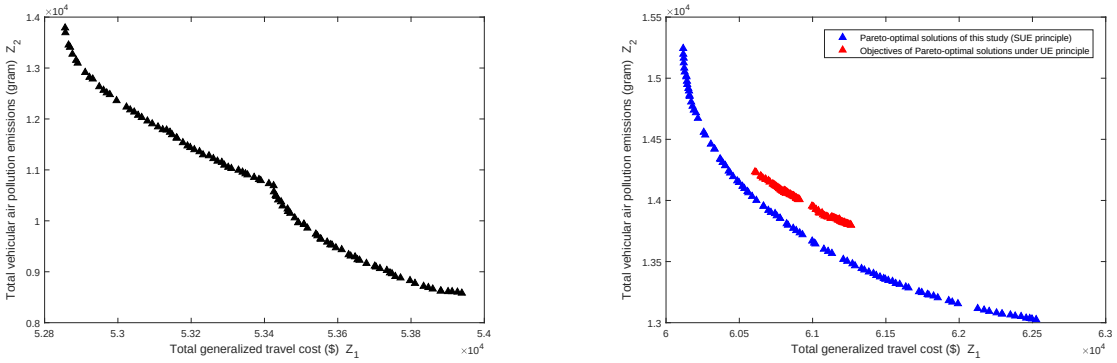

(a) Pareto-optimal solutions for the comparative experiment (UE principle)

(b) Value of objective functions for Pareto-optimal solutions under UE and SUE principle

Figure 9: Pareto-optimal solutions for the compensation optimization problem under UE and SUE principle

It comes to the conclusion by comparison that all Pareto-optimal solutions calculated by the new ridesharing compensation optimization model under the UE principle are dominated by the Pareto-optimal solutions of this study. As illustrated in Figure 9(a) and Figure 9(b), the neglect of limited perceived ability of travelers will cause policy-makers to overestimate the urban traffic system performance (i.e., underestimate the total generalized travel cost and total vehicular air pollution emissions) for same decision-making strategy of ridesharing compensation. As a result, the compensation optimization model which integrates travelers' choice behavior based on the UE principle can only provide a set of non-optimal decision-making strategies of ridesharing

compensation to traffic managers and policy-makers. Namely, by integrating travelers' choice behavior based on the SUE principle in the ridesharing compensation optimization model, this study derives a series of more effective decision-making strategies of ridesharing compensation.

Besides, the assumption that one ridesharing driver can only pick up one rider is widely adopted by previous studies as described in Section 1. Here, to analyze the effect of the value of ridesharing capacity on the decision-making problem of ridesharing compensation, two more comparative experiments have been conducted in which the capacity of ridesharing vehicle is equal to 1 and 2 (i.e., $Cap = 1, 2$) respectively. keep all other parameters unchanged. By solving the corresponding ridesharing compensation optimization model, we can obtain the Pareto-optimal solutions and the Pareto-efficient frontier for the two comparative experiments as shown in Figure 10. Similarly, we take the Pareto-efficient frontier of this study as a benchmark.

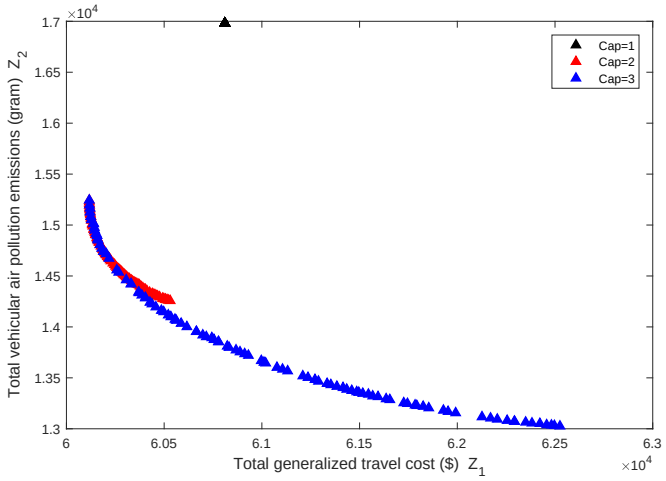

Figure 10: Pareto-efficient frontier for the compensation optimization problem under $Cap = 1, 2, 3$

For the ridesharing compensation optimization model in Eqs.(76-98), increasing the value of ridesharing capacity Cap means relaxing the constraints in Eqs.(90-91) and expanding the solution space of the optimization model in fact from the perspective of mathematical models. Therefore, as illustrated in Figure 10, the numerical experiment with $Cap = 3$ has the optimal Pareto-efficient frontier, then the numerical experiment with $Cap = 2$ has the suboptimal Pareto-efficient frontier, at last, the numerical experiment with $Cap = 1$ has the worst objective values. It means that the assumption one ridesharing driver can only pick up one rider will lead policy-makers can not make the optimal decision on the pricing problem of ridesharing compensation. Specifically, $Cap = 1$ means the number of ridesharing drivers should be equal to the number of ridesharing riders for each path between all OD pairs, i.e., $f_{p_3^{r1_s}} + f_{p_3^{r0_s}} = f_{p_2^{r1_s}}$. Thus, the path flow under generalized stochastic equilibrium always reaches saturated conditions. After given one optimal solution of ridesharing compensation $\boldsymbol{\tau} = \{5.26, 14.08, 13.13, 8.25\}$ and $\boldsymbol{\lambda}$, we can derive that the basic ridesharing compensation $\boldsymbol{\tau}$ varies in the range of $(-\infty, +\infty)$ will not change the actual ridesharing payment and compensation, the generalized stochastic user equilibrium, the total generalized travel cost, and the vehicular air pollution emissions. This is the reason why the numerical experiment with $Cap = 1$ has only one Pareto-optimal solution illustrated by the black

point in Figure 10. For the numerical experiment with $Cap = 2$, compared with the numerical experiment with $Cap = 3$, it has a smaller solution space. Thus, as illustrated in Figure 10, a part of its Pareto-optimal solutions have the same objective values as the Pareto-optimal solutions for the numerical experiment with $Cap = 3$, and most of its Pareto-optimal solutions are dominated by the Pareto-optimal solutions for the numerical experiment with $Cap = 3$. It indicates, generally, increasing the capacity that one ridesharing driver can pick up will improve the urban traffic conditions and pollution emissions simultaneously under Pareto-optimal solutions of ridesharing compensation.

6 Conclusions

This paper firstly develops a path-based generalized SUE model to describe heterogenous travelers' mode and route choice behavior in the presence of ridesharing programs. The path-based modeling method makes our study possible to overcome inherent shortcomings of the link-based formulation. Besides, we relax the assumption that each traveler owns a private vehicle and travelers can perceive the actual travel cost exactly to the more realistic scenario where travelers are heterogeneous in terms of car ownership and VOT, and they all have the limited perceived ability. As one of the main travel modes of non-car owners, public transit is considered in the formulation. Due to the inseparable and asymmetric travel cost functions, the proposed model is formulated as variational inequalities and an equivalent mixed complementarity problem.

Then, we address a decision-making problem of ridesharing compensation from the perspective of traffic managers and policy-makers who want to achieve total travel cost minimization and vehicular air pollution emissions minimization simultaneously. A bi-objective bi-level optimization model is proposed to formulate this decision-making problem, in which travelers' mode and route choice behavior has been respected. It is further reformulated as a mathematical problem with complementarity constraints and solved by an improved Non-Dominated Sorting Genetic Algorithm II to generate a set of Pareto-optimal solutions instead of one single solution for policy-makers. Finally, several numerical experiments based on two different-scale networks are carried out to demonstrate the validity of the proposed model.

Based on the works accomplished above, our analysis yields some interesting insights. First, when the urban traffic system reaches the generalized stochastic user equilibrium and path flow reaches saturated conditions, adjusting the basic ridesharing payment/compensation within a certain range will not change the actual ridesharing payment for each rider and the actual ridesharing compensation for each driver. Second, compared with ridesharing drivers, ridesharing subsidies are more attractive to ridesharing riders. Moreover, there is a significant improvement in urban traffic conditions and a slight decrease in vehicular air pollution emissions at the cost of huge subsidies provided by TNCs, but high-intensity subsidies are not a continuous and sustainable way to promote the development of ridesharing services. Third, the neglect of the limited perceived ability of travelers will cause policy-makers to overestimate the urban traffic system performance (i.e., underestimate the total generalized travel cost and total vehicular air pollution emissions) for the same decision-making strategy of ridesharing compensation. By integrating travelers' choice behavior based on the SUE principle instead of the UE principle in the ridesharing compensation optimization model, this study derives a series of more effective

decision-making strategies of ridesharing compensation.

Because ridesharing riders can enjoy a door-to-door travel service and do not have to bear the high cost of owning a private vehicle, ridesharing programs reducing the demand for private vehicles in the long run. Therefore, future work may involve exploring the optimal car ownership in the urban traffic system with the introduction of ridesharing programs. Besides, as for the equilibrium problem of ridesharing systems, all previous studies focus on the static equilibrium modeling problem, we will focus on the day-to-day dynamic stochastic user equilibrium problem for the urban traffic system with ridesharing programs to determine whether a stable state exists or not in the daily travel.

Acknowledgements

This work was supported by the National Natural Science Foundation of China (71901007), and China Postdoctoral Science Foundation funded project (BX20190022, 2019M650412).

References

Ban, J. X., Liu, H. X., Ferris, M. C. and Ran, B. (2006), 'A general mpcc model and its solution algorithm for continuous network design problem', *Mathematical & Computer Modelling An International Journal* **43**(5), 493–505.

Bimpikis, K., Candogan, O. and Saban, D. (2019), 'Spatial pricing in ride-sharing networks', *Operations Research* .

Brook, A., Kendrick, D. and Meeraus, A. (1988), 'GAMS, a user's guide', *ACM Signum Newsletter* **23**(3-4), 10–11.

Caulfield, B. (2009), 'Estimating the environmental benefits of ride-sharing: A case study of dublin', *Transportation Research Part D: Transport and Environment* **14**(7), 527–531.

Chen, Y. (2018), The impact of peer-to-peer ridesharing on travel mode: Empirical study of Uber effects on travel mode in Seattle, PhD thesis.

Concas, S. and Winters, P. L. (2007), 'Impact of carpooling on trip-chaining behavior and emission reductions', *Transportation research record* **2010**(1), 83–91.

Coulombel, N., Boutueil, V., Liu, L., Viguié, V. and Yin, B. (2019), 'Substantial rebound effects in urban ridesharing: Simulating travel decisions in paris, france', *Transportation Research Part D: Transport and Environment* **71**, 110–126.

Deb, K., Pratap, A., Agarwal, S. and Meyarivan, T. (2002), 'A fast and elitist multiobjective genetic algorithm: Nsga-ii', *IEEE transactions on evolutionary computation* **6**(2), 182–197.

Di, X., Ma, R., Liu, H. X. and Ban, X. J. (2018), 'A link-node reformulation of ridesharing user equilibrium with network design', *Transportation Research Part B: Methodological* **112**, 230–255.

Facchinei, F. and Pang, J.-S. (2007), *Finite-dimensional variational inequalities and complementarity problems*, Springer Science & Business Media.

Furuhata, M., Dessouky, M., Ordóñez, F., Brunet, M.-E., Wang, X. and Koenig, S. (2013), 'Ridesharing: The state-of-the-art and future directions', *Transportation Research Part B: Methodological* **57**, 28–46.

Gärling, T. and Steg, L. (2007), *Threats from car traffic to the quality of urban life: Problems, causes, and solutions*, Elsevier Amsterdam.

Harker, P. T. and Pang, J.-S. (1990), 'Finite-dimensional variational inequality and nonlinear complementarity problems: a survey of theory, algorithms and applications', *Mathematical programming* **48**(1-3), 161–220.

Jacobson, S. H. and King, D. M. (2009), 'Fuel saving and ridesharing in the us: Motivations, limitations, and opportunities', *Transportation Research Part D: Transport and Environment* **14**(1), 14–21.

Javid, R. J., Nejat, A. and Hayhoe, K. (2017), 'Quantifying the environmental impacts of increasing high occupancy vehicle lanes in the united states', *Transportation research part D: transport and environment* **56**, 155–174.

Larsson, T. and Patriksson, M. (1999), 'Side constrained traffic equilibrium models—analysis, computation and applications', *Transportation Research Part B: Methodological* **33**(4), 233–264.

Li, T. and Liu, Y. (2020), Mode choices and optimal car ownership of stochastic user equilibrium with ridesharing, Technical report.

Li, T., Sun, H., Wu, J. and Ge, Y.-e. (2017), 'Optimal toll of new highway in the equilibrium framework of heterogeneous households' residential location choice', *Transportation Research Part A: Policy and Practice* **105**, 123–137.

Li, Y., Liu, Y. and Xie, J. (2020), 'A path-based equilibrium model for ridesharing matching', *Transportation Research Part B: Methodological* **138**, 373–405.

Li, Z.-C. and Peng, Y.-T. (2016), 'Modeling the effects of vehicle emission taxes on residential location choices of different-income households', *Transportation Research Part D: Transport and Environment* **48**, 248–266.

Liu, Y. and Li, Y. (2017), 'Pricing scheme design of ridesharing program in morning commute problem', *Transportation Research Part C: Emerging Technologies* **79**, 156–177.

Long, J., Tan, W., Szeto, W. and Li, Y. (2018), 'Ride-sharing with travel time uncertainty', *Transportation Research Part B: Methodological* **118**, 143–171.

Ma, J., Xu, M., Meng, Q. and Cheng, L. (2020), 'Ridesharing user equilibrium problem under od-based surge pricing strategy', *Transportation Research Part B: Methodological* **134**, 1–24.

Nguyen, S. and Dupuis, C. (1984), 'An efficient method for computing traffic equilibria in networks with asymmetric transportation costs', *Transportation Science* **18**(2), 185–202.

Nielsen, J. R., Hovmøller, H., Blyth, P.-L. and Sovacool, B. K. (2015), 'Of "white crows" and "cash savers:" A qualitative study of travel behavior and perceptions of ridesharing in Denmark', *Transportation Research Part A: Policy and Practice* **78**, 113–123.

Noruzoliaee, M., Zou, B. and Liu, Y. (2018), 'Roads in transition: Integrated modeling of a manufacturer-traveler-infrastructure system in a mixed autonomous/human driving environment', *Transportation Research Part C: Emerging Technologies* **90**, 307–333.

Szeto, W. Y. and Jiang, Y. (2014), 'Transit route and frequency design: Bi-level modeling and hybrid artificial bee colony algorithm approach', *Transportation Research Part B: Methodological* **67**, 235–263.

Wang, J.-P., Ban, X. J. and Huang, H.-J. (2019), 'Dynamic ridesharing with variable-ratio charging-compensation scheme for morning commute', *Transportation Research Part B: Methodological* **122**, 390–415.

Wang, X., Yang, H. and Zhu, D. (2018), 'Driver-rider cost-sharing strategies and equilibria in a ridesharing program', *Transportation Science* .

Wang, Z., Chen, X. and Chen, X. M. (2019), 'Ridesplitting is shaping young people's travel behavior: Evidence from comparative survey via ride-sourcing platform', *Transportation research part D: transport and environment* **75**, 57–71.

Wardrop, J. G. (1952), 'Road paper. some theoretical aspects of road traffic research.', *Proceedings of the institution of civil engineers* **1**(3), 325–362.

Xu, H., Lou, Y., Yin, Y. and Zhou, J. (2011), 'A prospect-based user equilibrium model with endogenous reference points and its application in congestion pricing', *Transportation Research Part B: Methodological* **45**(2), 311–328.

Xu, H., Ordóñez, F. and Dessouky, M. (2015), 'A traffic assignment model for a ridesharing transportation market', *Journal of Advanced Transportation* **49**(7), 793–816.

Xu, H., Pang, J.-S., Ordónez, F. and Dessouky, M. (2015), 'Complementarity models for traffic equilibrium with ridesharing', *Transportation Research Part B: Methodological* **81**, 161–182.

Yan, C.-Y., Hu, M.-B., Jiang, R., Long, J., Chen, J.-Y. and Liu, H.-X. (2019), 'Stochastic ridesharing user equilibrium in transport networks', *Networks and Spatial Economics* pp. 1–24.

Yin, Y. and Lawphongpanich, S. (2006), 'Internalizing emission externality on road networks', *Transportation Research Part D: Transport and Environment* **11**(4), 292–301.